

DISSOLUTION KINETICS OF CUPRITE

IN SULPHURIC ACID - HYDROGEN PEROXIDE SOLUTIONS

By

Blas Basilio Ivankovich

11357-40

ProQuest Number: 10781991

All rights reserved

INFORMATION TO ALL USERS

The quality of this reproduction is dependent upon the quality of the copy submitted.

In the unlikely event that the author did not send a complete manuscript and there are missing pages, these will be noted. Also, if material had to be removed, a note will indicate the deletion.



ProQuest 10781991

Published by ProQuest LLC (2018). Copyright of the Dissertation is held by the Author.

All rights reserved.

This work is protected against unauthorized copying under Title 17, United States Code
Microform Edition © ProQuest LLC.

ProQuest LLC.
789 East Eisenhower Parkway
P.O. Box 1346
Ann Arbor, MI 48106 – 1346

A thesis submitted to the Faculty and the Board of Trustees of the Colorado School of Mines in partial fulfillment of the requirements for the degree of Master of Science in Metallurgical Engineering.

Signed: B. Tractonics

Golden, Colorado

Date: 5 JUNE, 1975

Approved: D.F. Bayler on behalf of
G.P. Martins G.P.M.
Thesis Advisor

William M. Mueller

W.M. Mueller
Head, Department of
Metallurgical
Engineering

Golden, Colorado

Date: 5 June, 1975

ARTHUR LAKES LIBRARY
COLORADO SCHOOL of MINES
GOLDEN, COLORADO 80401

ABSTRACT

The rate of dissolution of cuprite (Cu_2O) in sulphuric acid - hydrogen peroxide solutions was studied using the rotating disk technique. For H_2O_2 concentrations of 0.118 - 1.353 mol/liter, and H^+ concentrations of 0.07 - 0.86 mol/liter (0.05 - 0.80 mol/liter H_2SO_4) at 20°C and 800 RPM, the rate controlling reactions were found to be:

- (1) Removal of oxygen from the Cu_2O lattice by H^+ (anodic site)
- (2) Reduction of H_2O_2 (cathodic site).

The temperature sensitivity of the anodic and cathodic reactions was characteristic of a chemical controlled process, although neither the anodic nor the cathodic reaction was completely rate limiting. The dissolution rate was found to be independent of speed of rotation above 400 RPM. A rate expression fitting the experimental data was found from the proposed mechanism.

CONTENTS

LIST OF FIGURES

ACKNOWLEDGEMENTS	Page
CHAPTER 1. INTRODUCTION	1
1.1 Scope of the Problem	2
1.2 Present Investigation	3
CHAPTER 2. LITERATURE REVIEW	5
2.1 Pickling of Copper Wire	5
2.2 Dissolution Kinetics	8
2.3 Rotating Disk Studies	12
CHAPTER 3. THEORETICAL	14
3.1 Heterogeneous Reactions	14
3.1.1 Primary Steps	15
3.1.2 Kinetic Behavior Types	16
3.1.3 Rotating Disk Kinetics	21
3.2 Dissolution of Cu_2O	22
3.3 Hydrogen Peroxide Behavior	22
3.3.1 H_2O_2 Decomposition by Cupric Ions	23
3.3.2 H_2O_2 Stabilization	25
CHAPTER 4. EXPERIMENTAL	27
4.1 Dissolution Equipment	27
4.2 Cu_2O Disk Preparation	31
4.3 Reagents Used	32

	Page
4.4 Chemical Analysis	32
4.5 Run Procedure	33
CHAPTER 5. RESULTS AND DISCUSSION	36
5.1 Analysis of the Parameter	40
5.1.1 Hydrogen Ion Concentration	40
5.1.2 H ₂ O ₂ Concentration	40
5.1.3 Rotation Speed	41
5.1.4 Temperature	41
CHAPTER 6. CONCLUSION	56
APPENDIX 1	59
APPENDIX 2	79
REFERENCES	84

LIST OF FIGURES

Figure	Page
3.1 Partial Eh-pH diagram describing the Cu_2O disproportionation	24
4.1 General view of the equipment showing the reactor assembly, temperature bath, recorder and motor speed controller	28
4.2 Disk holder set up, and reactor with water jacket mounted in place	29
4.3 Disk holder sketch showing the two part assembly and the mean dimentions	30
4.4 Copper disks before and after dissolution.	35
5.1 Relation between measured H_2SO_4 and H^+ in solution	38
5.2 Typical behavior of the Cu_2O dissolution, and complete zero order plot for a reacted disk .	39
5.3 Effect of the $\{\text{H}^+\}$ concentration on the dissolution rate, the continuous lines are the fitted values from the rate equation, the points represent the experimental data	42
5.4 Effect of the H_2O_2 concentration on the dissolution rate. The continuous lines are the predicted value from the rate equation	43
5.5 Effect of the speed of rotation on the dissolution of Cu_2O : 0.86 mol/liter H^+ , 0.471 mol/liter H_2O_2 , 20°C	45
5.6 Effect of the speed of rotation on the dissolution of Cu_2O : 0.438 mol/liter H^+ , 0.235 mol/liter H_2O_2 , 20°C	46
5.7 Effect of temperature on the dissolution of Cu_2O : 0.86 mol/liter H^+ , 0.471 mol/liter H_2O_2 , 800 RPM .	48
5.8 Log rate of reaction vs. reciprocal of temperature for the dissolution of Cu_2O : 0.86 mol/liter H^+ , 0.471 mol/liter H_2O_2 , 800 ² RPM	49

Figure	Page
5.9 Effect of temperature on the dissolution of Cu_2O : 0.122 mol/liter H^+ , 0.706 mol/liter H_2O_2 , 800 RPM	50
5.10 Log rate of reaction vs. reciprocal of temperature for the dissolution of Cu_2O : 0.122 mol/liter H^+ , 0.706 mol/liter H_2O_2 , 800 ² RPM	51
5.11 Electrochemical representation of the Cu_2O dis- solution	53
A.1.1 Dissolution of Cu_2O in 0.235 mol/liter of H_2O_2 at different H^+ concentrations: 20°C, 800 RPM	70
A.1.2 Dissolution of Cu_2O in 0.353 mol/liter H_2O_2 at different H^+ concentrations.	71
A.1.3 Dissolution of Cu_2O in 0.471 mol/liter H_2O_2 , at different H^+ concentrations.	72
A.1.4 Dissolution of Cu_2O in 0.07 mol/liter H^+ at different concentrations of H_2O_2 : 20°C, 800 RPM	73
A.1.5 Dissolution of Cu_2O in 0.122 mol/liter H^+ at different concentrations of H_2O_2 : 20°C, 800 RPM	74
A.1.6 Dissolution of Cu_2O in 0.228 mol/liter H^+ at different concentrations of H_2O_2 : 20°C, 800 RPM	75
A.1.1 Tables of Copper Concentration as a Function of Time for the Dissolution Tests, Table 1.1-1.10	60-69

ACKNOWLEDGEMENTS

The author wishes to express his thanks and grateful recognition to Dr. G. P. Martins for his guidance and valuable advice throughout the course of this investigation. Thanks also go to the graduate students in the Department for their help and advice, and to Mrs. Cathy Moser for her valuable help in typing the thesis.

The advantages of the scholarship and financial support from Centromin Peru are recognized.

Chapter 1

INTRODUCTION

The pickling of metal products (wire, plates, tubes, etc.) to remove oxides formed by previous operations in order to obtain either a product of good appearance or physical properties, is a common operation in the metals industry. Such is the case in the drawing of copper wire for use in the manufacture of electrical cables.

Rigid specifications for the electrical conductivity and tensile strength of these products have to be maintained. These properties are severely affected, if oxides are present in the coil as a result of being "drawn in" during drawing of the copper wire. This is comparable to having a high level of impurities in the metal. Therefore, in this respect, the removal of oxides is of equal importance as the refining process.

The use of oxidants in acidic pickling solutions provide complete and faster removal of these oxides, thus allowing a clean copper surface to be obtained.

Common oxidants, such as $K_2Cr_2O_7$, $Na_2Cr_2O_7$, $Fe_2(SO_4)_3$, although effective, present pollution problems associated with the effluent solutions as well as reduction in the tool

life, as a result of contamination from the residual oxidant components remaining on the wire. The use of hydrogen peroxide as an oxidant appears to offer a solution to the problems previously mentioned.

1.1 Scope of the Problem

The general category into which the present investigation falls, is that of heterogeneous reaction systems: in particular, solid/aqueous solution systems. These include pure metal and metal compound dissolution, as well as the reduction of ionic species on the surface of a metal. Examples of these processes include corrosion, dissolution of minerals, electrolysis and cementation.

Fundamental concepts pertaining to this class of system are well established in the literature (1-5). Experimental studies using rotating disk electrodes to test these concepts are also numerous (6-12). The hydrodynamic behavior of the rotating disk and the coupled mass-transport associated therewith have been developed and redeveloped by numerous works (6,13).

The electrochemical nature of dissolution reactions and of cementation process has led to the development of numerous reaction mechanisms to describe these processes (14-15).

It is therefore sufficient to say that fundamental concepts, which are appropriated to the present investigation, are well documented in the literature.

The removal of copper oxides by pickling in acidic solutions has been reported primarily in conjunction with industrial processes (16-17) and, as such, does not cover the fundamental aspects of the process. In addition, the experiments reported are usually specific to the system tested. The use of hydrogen peroxide as an oxidant in the process has been reported (18), but the study was not carried out under controlled conditions. It is therefore difficult to postulate a mechanism and associated rate expression from these tests. The need for carefully controlled tests in order to accomplish these goals is at once apparent.

1.2 Present Investigation

The dissolution kinetics of cuprite (Cu_2O) in aqueous $\text{H}_2\text{SO}_4 - \text{H}_2\text{O}_2$ solutions, using the well established technique of the rotating disk, will be studied.

The particular conditions of interest are those in which copper, formed by the disproportionation of the Cu_2O , is absent from the surface.

The aim of this study is to find a possible reaction mechanism and rate expression which would provide a better understanding of the pickling process as well as allowing the process to be quantified.

The results of this study are presented in the following five chapters. In Chapter 2, pickling practice and references in dissolution kinetics are presented. Chapter 3

covers theoretical aspects of the dissolution kinetics. The experimental system is reported in Chapter 4. In Chapter 5, the results of the experiments conducted are given. These are then analyzed and discussed, leading to a proposed mechanism. The conclusion to the work is covered in Chapter 6, where conclusions deduced from the present work are noted together with suggestions for future work.

Chapter 2

LITERATURE REVIEW

This chapter is divided into three sections covering:

- (a) General aspects of the pickling process, and importance of the use of H_2O_2 as an oxidizing agent,
- (b) some examples in the field of metal/compound dissolution kinetics,
- (c) rotating disk studies.

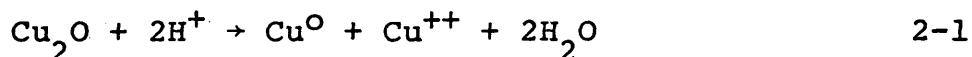
2.1 Pickling of Copper Wire

The pickling of copper is described elsewhere (16,17,18) as a process of removal of scales of oxides adhered to the metal during the hot rolling of copper wire bars. The wire-- most common diameters 5/16" and 9/16" -- subsequently undergoes drawing in order to obtain smaller gauge wire for electric cables. The scale is a double layer of oxides, CuO (cupric oxide) the outer, and Cu_2O (cuprous oxide) the inner and thicker one.

Industrially, the removal of these scales is carried out in two steps. In the first step, the thin layer of CuO present is dissolved in hot ($65^{\circ}C$) concentrated sulphuric acid (10-25% by volume). These conditions are required, since the dissolution rate would otherwise be very low at low

temperatures or with low concentration of sulphuric acid. The surface of the wire after this pre-pickling treatment is covered by a red scale formed by metallic copper, and remaining undissolved oxides, mainly Cu_2O . This red scale is then removed by a sulphuric acid - H_2O_2 pickling treatment.

Sulphuric acid appears to be the most common agent for the removal of scales adhering to the copper wire. The disadvantage in using this acid medium alone is that the dissolution results in the disproportionation of the Cu_2O , thereby producing metallic copper according to the overall reaction:

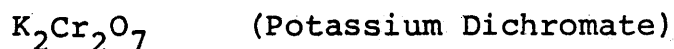


The copper produced may be removed using high pressure jets during rinsing. However, this is not totally efficient, and its presence along with Cu_2O remaining will cause problems during the next treatment step. These include:

(a) Inclusion of scale in the wire during drawing, reducing the electrical conductivity and tensile strength.

(b) The presence of the scale also results in lubricant contamination, reducing the working life of the drawing dies.

Consequently the use of oxidizing agents, which completely remove this scale, is essential. The following have been used industrially:



$\text{Na}_2\text{Cr}_2\text{O}_7$	(Sodium Dichromate)
$\text{Fe}_2(\text{SO}_4)_3$	(Ferric Sulfate)
H_2O_2	(Hydrogen Peroxide)

In the last few years, the use of H_2O_2 as an alternative to the other products has increased. The attractiveness of H_2O_2 for use in this process comes from the ease of treatment of the solutions resulting after pickling. In particular, this product leaves no impurities as is the case when $\text{K}_2\text{Cr}_2\text{O}_7$ and $\text{Na}_2\text{Cr}_2\text{O}_7$ are used, which produce additional metal ions in solution. These metal ions are difficult to remove from the effluent, and can produce water pollution when discarded. In addition the life of dies for the subsequent drawing is reduced, because of contamination of the lubricant.

The use of H_2O_2 is now possible because of the development of stabilizers which prevent its rapid decomposition, thereby making its use economically feasible.

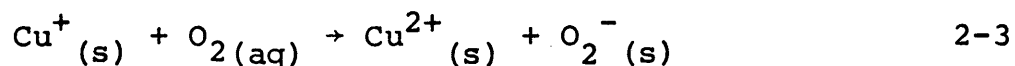
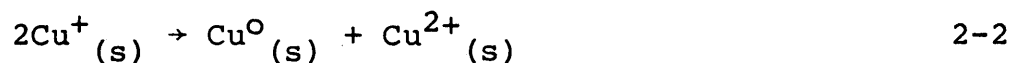
The conditions used in $\text{H}_2\text{SO}_4 - \text{H}_2\text{O}_2$ copper pickling are 10% by volume H_2SO_4 , 5-20 g/l H_2O_2 , 30-55°C. The average weight loss of copper, removed as scales, by this process, is 1.2 g/kg for wires of 5/16" diameter.

The solutions from the two pickling steps (CuO , Cu_2O) with concentrations of Cu^{++} and H_2SO_4 around 20-40 g/l and 100-150 g/l respectively go to copper recovery by either Electrowinning or Crystallization of $\text{CuSO}_4 \cdot 5\text{H}_2\text{O}$, the decopperized liquor being returned to the pickling tanks.

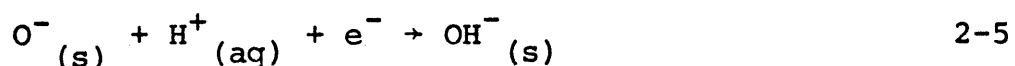
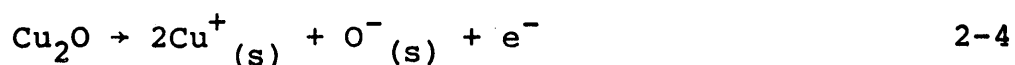
Following pickling, the descaled copper wire goes to a rinse treatment in which the remaining acid solution adhering to the wire is neutralized, and the Cu^{++} precipitated as hydroxide in the presence of basic solutions (NaOH , Na_2CO_3 , $\text{Cu}(\text{OH})_2$). In addition, any H_2O_2 present is eliminated by decomposition into water and oxygen.

2.2 Dissolution Kinetics

Hauffe and Reinhold (32) have studied the dissolution of Cu_2O in low concentration solutions of H_2SO_4 and H_2O_2 , 10^{-3}N and from 10^{-3} to 10^{-2} moles/liter, respectively. They found that fixing the H_2SO_4 at the value given, the dissolution rate increased on increasing the H_2O_2 concentration up to 10^{-2} moles/liter. Additional amounts did not affect the rate. They also made an attempt to explain the mechanism of the dissolution of Cu_2O in the presence of oxygen and H_2SO_4 , proposing that the following competing reactions account for the dissolution:



The subscript (s) indicates that species are located on the surface. The $\text{Cu}^+_{(s)}$ comes from the reaction:



Reaction (2-3) was assumed to be feasible because of the ability of oxygen to accept electrons from the valence band of the p-type semi-conductor, according to:



They explained the absence of Cu on the surface by saying that either reaction (2-2) is suppressed by reaction (2-3) or that the copper formed is rapidly oxidized by the oxygen.

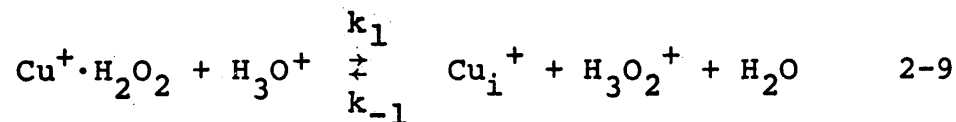
Colcleugh and Grayson (33), using a rotating cylinder, studied the dissolution rate of copper in deaerated solutions in the presence of low concentrations of H_2O_2 and sulphuric acid. One of their findings was that there exists a linear relationship between Hydronium ion $\{\text{H}_3\text{O}^+\}$ concentration and the inverse of the rate coefficient k , establishing the equation:

$$k = \frac{k_1}{k_2 + \{\text{H}_3\text{O}^+\}} \quad 2-7$$

where k is the rate coefficient for the overall rate expression:

$$\frac{d\{\text{Cu}^{++}\}}{dt} = k\{\text{Cu}^{++}\}^{\frac{1}{2}}\{\text{H}_2\text{O}_2\} \quad 2-8$$

they proposed that the step reaction:

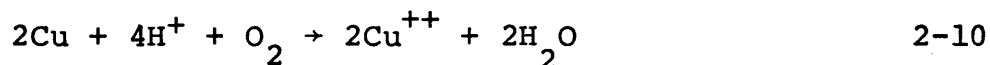


represents the inhibition step, and responsible for type of

expression shown in (2-7).

Habashi (14), using an electrochemical model which assumes the presence of anodic and cathodic areas on the surface of the "electrode", where the reaction takes place, explained the mechanism of the dissolution of copper in dilute sulphuric acid in the presence of oxygen. He showed that the total rate is obtained by adding two separate reactions:

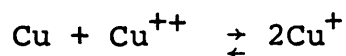
1. Corrosion reaction-for the overall reaction



and considering that the $\{\text{O}_2\}$ acts as a depolarizer and $\{\text{H}^+\}$ as a complexing agent which prevents the formation of hydrolytic products, he found that the rate of reaction (e.g. moles of Cu^{++} per unit time) is given by:

$$\text{Rate} = \frac{k_1 k_2 A \{\text{O}_2\} \{\text{H}^+\}}{k_1 \{\text{O}_2\} + k_2 \{\text{H}^+\}} \quad 2-11$$

2. Autocatalytic reaction



with rate expression (e.g. moles of Cu^{++} per unit time)

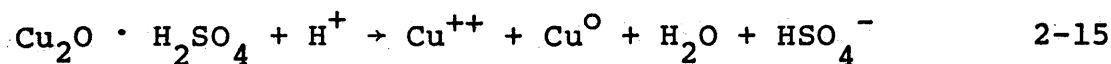
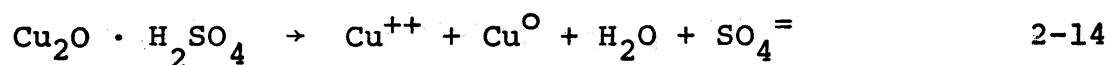
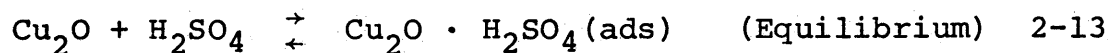
$$\text{Rate} = k'' \{\text{Cu}^{2+}\}^{\frac{1}{2}}$$

In this reaction the copper(I) reacts rapidly with the oxygen, regenerating the copper(II) so the total rate becomes:

$$\text{Rate} = \frac{k_1 k_2 A \{O_2\} \{H^+\}}{k_1 \{O_2\} + k_2 \{H^+\}} + k'' \{Cu^{2+}\}^{\frac{1}{2}} \quad 2-12$$

It was demonstrated that initially, when the concentration of Cu^{2+} is small, the second term of the rate expression is negligible compared to the first, therefore the rate simplifies to the first term only. At high concentration of Cu^{++} the overall expression reduces to only the second term. He also used similar models to explain the kinetics of dissolution of copper, silver and gold in potassium cyanide in the presence of oxygen.

Wadsworth and Wadia(34) studied the dissolution of Cu_2O in sulphuric acid solutions in the absence of oxygen using Cu_2O plates obtained by oxidized copper. They explained their experimental results by proposing two rate reactions and one equilibrium hydrolytic adsorption reaction:



The dissolution was found to be independent of the stirring rate and with an activation energy of 10.5 kcal/mol. The total rate proposed ($mg\ Cu^{++}\ cm^{-2}\ min^{-1}$) at $31^\circ C$ was:

$$R_T = \frac{1.59 \times 10^6 \{H_2SO_4\}}{1 + 1.59 \times 10^6 \{H_2SO_4\}} (0.523 \{H^+\} + 0.290) \quad 2-16$$

$\{H_2SO_4\}$ expresses the amount of H_2SO_4 undissociated, and for the conditions used, varied from 7.79×10^{-6} to 1.69×10^{-3} moles, as the total molarity of sulphuric acid in the system varied from 0.103 to 1.377. It is interesting to note that the premultiplying factor of the equation given only varies between 0.92 and 1 for the range of free H_2SO_4 encountered (the smaller value corresponding to the lower concentration)

C. V. King (22), in studying the dissolution of Fe in hydrochloric acid using H_2O_2 as depolarizer, found that the rate varies with the H_2O_2 concentration almost linearly up to 0.12 molar of H_2O_2 for a fixed concentration of HCl (0.05N). Further increase in H_2O_2 causes the rate to fall. He explained this behavior by mentioning the formation of films on the surface. The exact nature of these films was not revealed. Whether they are products resulting from solid precipitation, or adsorbed oxygen (O_2^-) or any other anion on the surface which act as a blind, is not clear. Gatos (11), observed the same behavior in the dissolution of semiconductors such as InSb and GaSb. He interpreted this finding by postulating that the dissolution is carried out by the pores of the film.

2.3 Rotating Disk Studies

The use of rotating disk technique in the dissolution of metals and their compounds has increased in recent years. Although no work using Cu_2O has been reported, metals such as Cu, Zn and Fe have been studied in some detail. These

studies support the contention that this method is well suited to the investigation of heterogeneous reactions, and particularly those which are controlled by transport of species to or from the interphase. A compilation of papers on copper dissolution was presented by Krebs(24) in his thesis on the "Dissolution Kinetics of Copper in Hydrochloric Acid" among those Gregory and Riddeford(7) working in the dissolution of copper in sulphuric acid solutions pointed out that the type of depolarizer used has a strong influence on the type of control. Examples of the behavior of O_2 , ferric salts and p-benzoquinone on the kinetics of Cu dissolution, when using potassium dichromate as depolarizer (3×10^{-2} molar $K_2Cr_2O_7$, 1.0 molar H_2SO_4 , $20^\circ C$) were cited. They found that the process is completely controlled by the diffusion of dichromate ions to the surface. However, at concentrations of sulphuric acid equivalent to an initial acid/dichromate ratio of less than 7, the reaction was no longer first order with respect to dichromate; this apparently being due to starvation of H_2SO_4 .

Chapter 3

THEORETICAL

In the following sections general aspects of the theory relevant to the process of Cu_2O dissolution will be given. These include principles of heterogeneous reactions, together with a description of the features of the rotating disk electrode.

Thermodynamic considerations on the dissolution of Cu_2O in the absence and presence of H_2O_2 , based on the Eh-pH diagram, together with an explanation of the homogeneous decomposition catalysis of the H_2O_2 , and methods of preventing this from occurring, will complete this chapter.

3.1 Heterogeneous Reactions

Processes of this kind are characterized by the presence of more than one phase in the system under study. Although some slow step in the overall process could be homogeneous (e.g. diffusion processes, or the products distributed in only one phase), it is the presence of more than one phase taking part in the reaction which constitutes a heterogeneous system.

In the present study a solid phase (Cu_2O) is in contact with an aqueous medium ($\text{H}_2\text{O}-\text{H}_2\text{SO}_4-\text{H}_2\text{O}_2$) into which Cu^{++}

is transferred. This overall process is the result of a number of sequential steps which will now be described.

3.1.1 Primary Steps - The dissolution kinetics of a solid can involve the following two processes:

- (a) Transport processes,
- (b) Any chemical interaction on the surface which brings about transformation of the solid phase (chemical processes).

The transport processes are related only to the behavior of the species in solution, in particular the diffusion and convective phenomena occurring in the liquid. The convective phenomena are a result of the motion of the solution and their influence can extend all the way to the solid/liquid interphase.

The relative effects of these two transport processes were demonstrated, for the case of a rotating disk, by Levich (13), with the aid of the Peclet number $v_0 L/D$, where v_0 is the characteristic flow velocity in the system; L is the characteristic length associated with the boundary layer and D is the diffusion coefficient. For high Peclet number, the velocity is large compared to the diffusion coefficient, consequently the transport process will be controlled by convection. When the velocity is small compared to the diffusion coefficient, molecular diffusion becomes the primary transport step. This can be seen from the simplified diffusion equation for the system at steady state:

$$D \frac{d^2c}{dx^2} - v_x \frac{dc}{dx} = 0 \quad 3.1$$

At high velocities the first term becomes negligible compared to the second, and the solution to the equation yields a uniform concentration. When the second term becomes negligible at low velocities, a linear concentration profile is obtained in the boundary layer.

It should be apparent, therefore, that in general two transport steps have to be considered:

- (1) Convective transport is associated with the motion of the liquid and is responsible for the transfer of the species of interest from the bulk to the surface or to the boundary layer.
- (2) Transport by molecular diffusion is associated with the concentration gradient of soluble reactants or products and quite often is confined to the boundary layer.

In the case of the chemical processes, the surface of the material undergoing reaction plays the most important role. It is here that the reactants are reduced or oxidized. In addition other types of activation could be produced by adsorption of reactants on the surface. Thus, the chemical processes may be separated to include three additional steps:

- (3) Adsorption of reactants
- (4) Chemical reaction on the surface
- (5) Desorption of the products

3.1.2 Kinetic Behavior Types- One or more of the steps considered may be rate-controlling, and classification into three types may be made, thus:

(a) Diffusion Control. This occurs when the chemical reaction at the surface is fast compared to the transport processes in the system. Under these conditions the overall process may become controlled by the diffusion of reactants through the boundary layer, to the interphase.

The approach to this kind of control is given by several publications (2-3, 19-21). On applying Fick's law of diffusion the following equation is obtained:

$$N_{Rx} = -D_R \frac{dC_R}{dx} \quad 3.2$$

This equation relates the diffusing flux of a reactant species R to the concentration gradient in the system. The diffusion coefficient D_R is the proportionality constant in this relationship. If it is assumed that the concentration profile in the boundary layer, thickness δ , is linear, and that the concentration of the reactant species at the interphase is negligible (instantaneous irreversible reaction), a mass balance on the system gives:

$$\frac{dC_R}{dt} = - \frac{d_{RA}}{v\delta} \cdot C_R \quad 3.3$$

Replacing $\frac{d_{RA}}{v\delta}$ by k , an apparent first order reaction expression is obtained:

$$- \frac{dC_R}{dt} = k \cdot C_R \quad 3.4$$

This expression is sometimes written as:

$$-\frac{dC_R}{dt} = k_T \cdot \frac{A}{v} \cdot C_R \quad 3.5$$

where $k_T = D/\delta$ is the rate coefficient for the transport controlled process.

Other characteristics for this kind of control are

(22):

(1) In the absence of deposits or films on the surface, for laminar flow, the rate of dissolution, using the same reactant concentration for different solids is the same.

(2) Since the thickness of the boundary layer δ , depends on the velocity of the system, an increase in speed reduces this thickness, resulting in higher rates.

(3) k_T is a function of D_R and the latter (for low concentration of the diffusing species) is linearly dependent on temperature by the Stokes-Einstein equation (3):

$$D = \frac{RT}{N} \cdot \frac{1}{2\pi r\eta} \quad 3.6$$

Processes of this type are less temperature sensitive than those controlled by chemical reaction.

(b) Chemical Control - For this type of control, the concentration gradient in the boundary layer is negligible, and no depletion of the reactants is assumed to exist.

The general rate equation, considering only the reactant

C_R and assuming an irreversible reaction is:

$$-\frac{dC_R}{dt} = k_C \{C_R\}^n \frac{A}{V} \quad 3.7$$

where k_C is the rate coefficient for chemical controlled processes, and n is the order of the reaction with respect to C_R . For this type of process, since the speed of rotation and fluid properties do not have any effect on the reaction surface, the rate is independent of speed, viscosity and diffusion coefficient.

The temperature sensitivity of either chemical or transport controlled processes can be measured, using the Arrhenius expression:

$$K = k_0 e^{-E/RT} \quad 3.8$$

where:

k_0 = frequency factor
 E = activation energy
 T = absolute temperature
 R = gas constant

On plotting $\log K$ vs. $1/T$ and finding the slope of the straight line drawn through the points the value $E/2.3R$ is obtained. As mentioned before and from the values of the activation energy, chemical controlled processes are more temperature sensitive ($E > 8$ kcal/mol) than those for transport ($E < 2-5$ kcal/mol).

(c) General Kinetics

Under this classification are those processes in which, both the chemical reaction and the convective-diffusion (transport) processes are important.

From the equations for transport and chemical control given before (3-5,7):

$$-\left. \frac{dC_R}{dt} \right|_C = K_C C_{R_i}^n \frac{A}{V} \quad 3.8$$

$$-\left. \frac{dC_R}{dt} \right|_T = K_T (C_R - C_{R_i}) \frac{A}{V} \quad 3.9$$

where C_{R_i} is the concentration of the R species at the surface, since in general this concentration is neither negligible nor equal to the bulk of the solution.

Considering a first order rate in the chemical process, then at steady state:

$$K_C C_{R_i} = K_T (C_R - C_{R_i}) \quad 3.10$$

Solving for C_{R_i} , and replacing in either equation 3.8 or 3.9, the resulting expression is:

$$-\left. \frac{dC_R}{dt} \right|_C = -\left. \frac{dC_R}{dt} \right|_T = \left[\frac{K_T}{1 + \frac{K_T}{K_C}} \right] \frac{A}{V} C_R \quad 3.11$$

Zembura (8), using the equations obtained by Levich (given in the next section) for the relationship between the transport controlled rate and angular velocity of a rotating disk, theoretically investigated the effect of quantity in the parentheses on the right side of the equation 3.11 as a function of angular velocity for various values of K_T/K_C . He showed that for K_T/K_C ratios between 1/5 and 10 general kinetics prevail. Thus, for ratios lower

than 1/5 it is possible to measure experimentally the diffusion of reactants.

3.1.3 Rotating Disk Kinetics

The rotating disk offers by its well defined parameters a better approach than those using other types of geometry, particularly in the sense that the conditions of transport of the reactants to any point at the surface are uniform.

The mathematical solution to the equation of continuity, motion and diffusion was solved by Levich (13), who obtained the following expression:

$$K_T = 0.62 D^{2/3} \omega^{1/2} \nu^{-1/6} \quad 3.12$$

where ω is the angular velocity of the disk and ν is the kinematic viscosity of the solution. Knowing the values for ν and D for the solution it is possible to define K_T . The value of δ (diffusion boundary layer thickness) was also found to be:

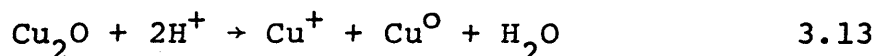
$$\delta = 1.805 D^{1/3} \nu^{1/6} \omega^{-1/2} \{0.8934 + 0.316 (D/\nu)^{0.36}\} \quad 3.13$$

Requirements for reproducible results using this method are:

- (a) Large diameter of the disk compared with δ
- (b) Large enough volume of solution to assure that the boundary layer does not interact with the vessel containing the solution.
- (c) Minimum eccentricity of the disk.

3.2 Dissolution of Cu_2O

Dissolution of Cu_2O in acid solutions in the absence of an oxidant results in a disproportionation reaction, because of the amphoteric character of the Cu_2O (25), resulting in two valence state products, one oxidized (Cu^{++}) and the other reduced (Cu°) according to:



A partial Eh-pH diagram in the region of interest explains this effect (Fig. 3.1).

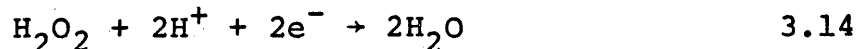
The lines $A_1\text{-O}$ and $A_2\text{-O}$ represent the oxidizing and reducing function of Cu_2O and the intersection O is the limit for its stability. To the left of this point the Cu_2O will disproportionate into Cu^{++} and Cu° . This occurs as a result of a decrease in pH. The extensions OA_1 and OA_2 therefore have no meaning and a new existence line OA_3 separating Cu^{++} and Cu° is obtained. In the presence of high oxygen potential, as is the case when using H_2O_2 , there are two possibilities:

(a) the Cu_2O may produce Cu° and Cu^{++} but since the stable species is the Cu^{++} , the copper oxidizes rapidly

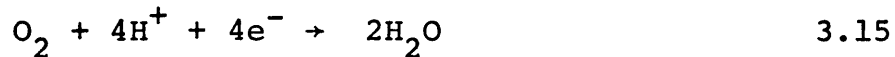
(b) the Cu_2O could alternatively produce Cu^{++} , inhibiting the formation of Cu° .

3.3 Hydrogen Peroxide Behavior

For the half cell reaction



the value of $E^{\circ}=1.76$ indicating the strong oxidizing power of the H_2O_2 agent, significantly higher than that for the O_2 reduction:

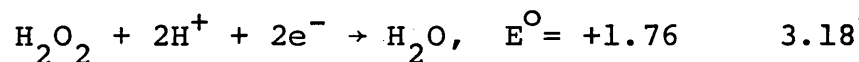
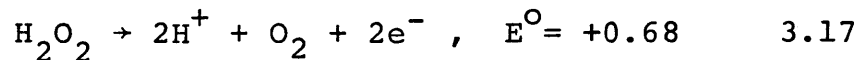


with $E^{\circ} = 1.229$.

H_2O_2 was found to be stable in solutions, in the absence of metallic ionic species, which produce homogeneous catalytic decomposition (26) e.g.- Fe^{++} , Fe^{+++} and Cu^{++} . Also a solid catalyst such as silver, Joksimovic - Tiapkin (27), produces the same effect, with the overall reaction being:



Behavior that is predicted considering the region of double instability given by the half cell reactions:



If the domain of any solid or dissolved species is located in between this region, the reaction (3.16) is likely to occur.

3.3.1 Hydrogen Peroxide Decomposition by Cupric Ions

The decomposition catalysis of the H_2O_2 by the presence of the Cu^{++} , will be discussed in relation to the pickling of copper, where the H_2O_2 is in contact with cupric ions for long periods of time. Because of the loss of H_2O_2 associated with this decomposition, its use as an

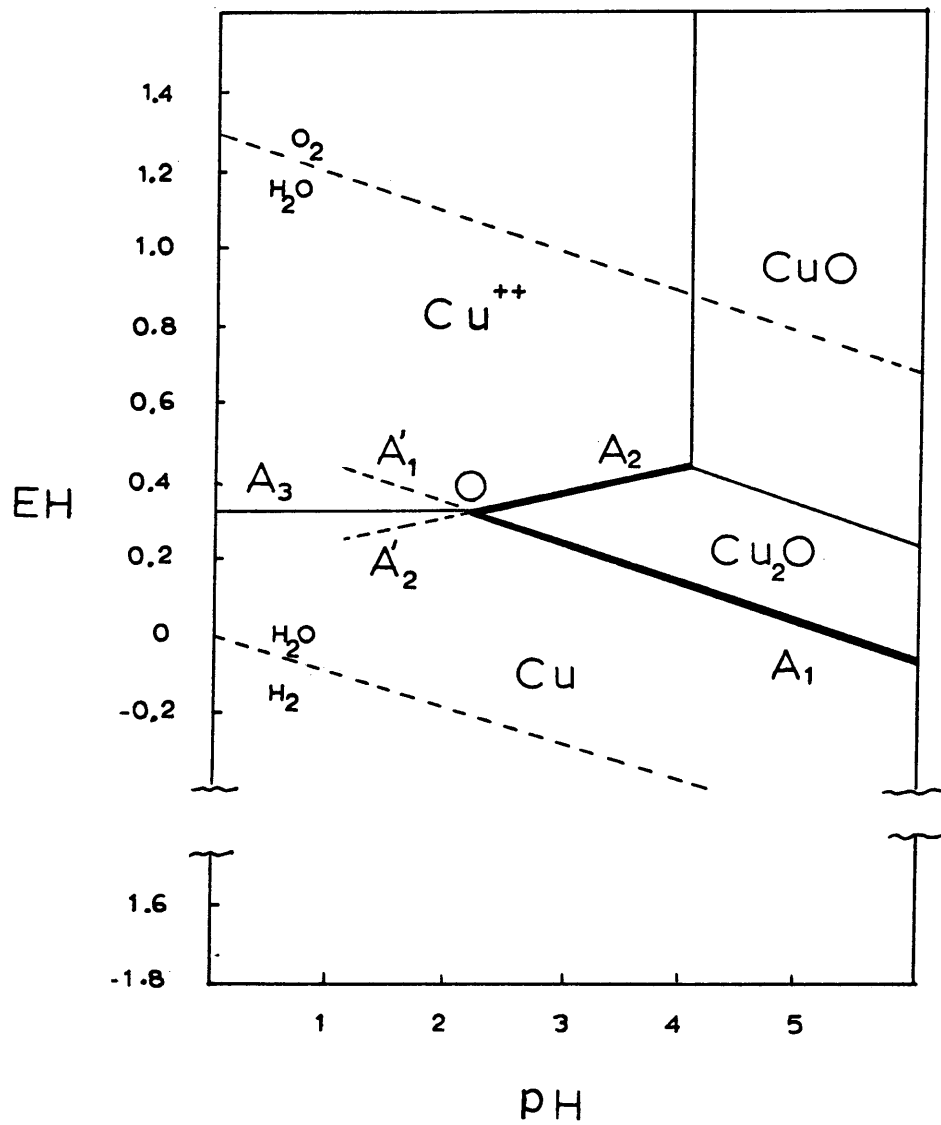
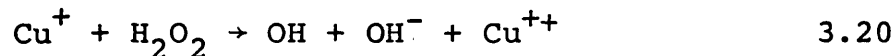
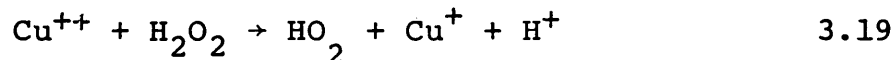


Fig. 3.1. Partial Eh-pH diagram describing the Cu_2O disproportionation: 1 mol/liter Cu^{++} , $25^{\circ}C$

oxidant has been questionable on economic grounds.

During the present investigation this effect was not experienced. However, the concentrations of cupric ion in solution and the time of reaction were quite small. The effect of cupric ions on the decomposition catalyses of the H_2O_2 has received only limited study, unlike the case for ferric and ferrous ions. Possible mechanisms for the cupric ion system are based on similarities with the latter system species. It has been suggested (28-29) that the reaction taking place involves the Cu^{++}/Cu^+ Redox system similar to the case of Fe^{+++}/Fe^{++} . The initial reactions to consider could be:



3.3.2 H_2O_2 Stabilization-

This process is as yet not well understood, and theories in which the formation of stable complexes with the catalyst responsible for the decomposition have gained some acceptance. This appears to be the case for organic phosphates and phosphites, e.g. dibutyl phosphate.

Lewis (30) stated that sodium stannate in solutions at pH between 3-5 forms negatively charged colloidal hydrous stannic oxides by hydrolysis, which absorb catalytic actions. The substances used as stabilizers are numerous. Some of

them are in actual use to stabilize the H_2O_2 in copper pickling are:

Dibutyl Phosphate
Ethane Sulfonic Acid
Tri-n-propanolamine
Propyl Sulphate

Chapter 4

EXPERIMENTAL

The study of the dissolution of Cu_2O , was carried out in a system consisting of a rotating disc of solid Cu_2O , immersed in an aqueous solution of H_2SO_4 and H_2O_2 with a liquid volume of 500 ml. In the sections which follow, a description of equipment and experimental details pertinent to the study is given.

4.1 Dissolution Equipment

The basic features of the equipment used may be illustrated by referring to the photographs in Figs. 4-1 and 4-2. It consisted of the following:

(a) A pyrex glass vessel of $4\frac{1}{2}$ -in. I.D. with a working capacity of 500 ml, mounted below a circular stainless steel plate.

The stainless steel plate was drilled and tapped to carry a bearing housing for the rotating disk assembly and ports for inserting a thermocouple, sampling tube, and for filling. This plate was mounted below a base plate with a $\frac{1}{4}$ H.P. variable speed D.C. motor, and provided with a spring coupling to drive the rotating disk.

(b) Two disk holders, one of stainless steel, and

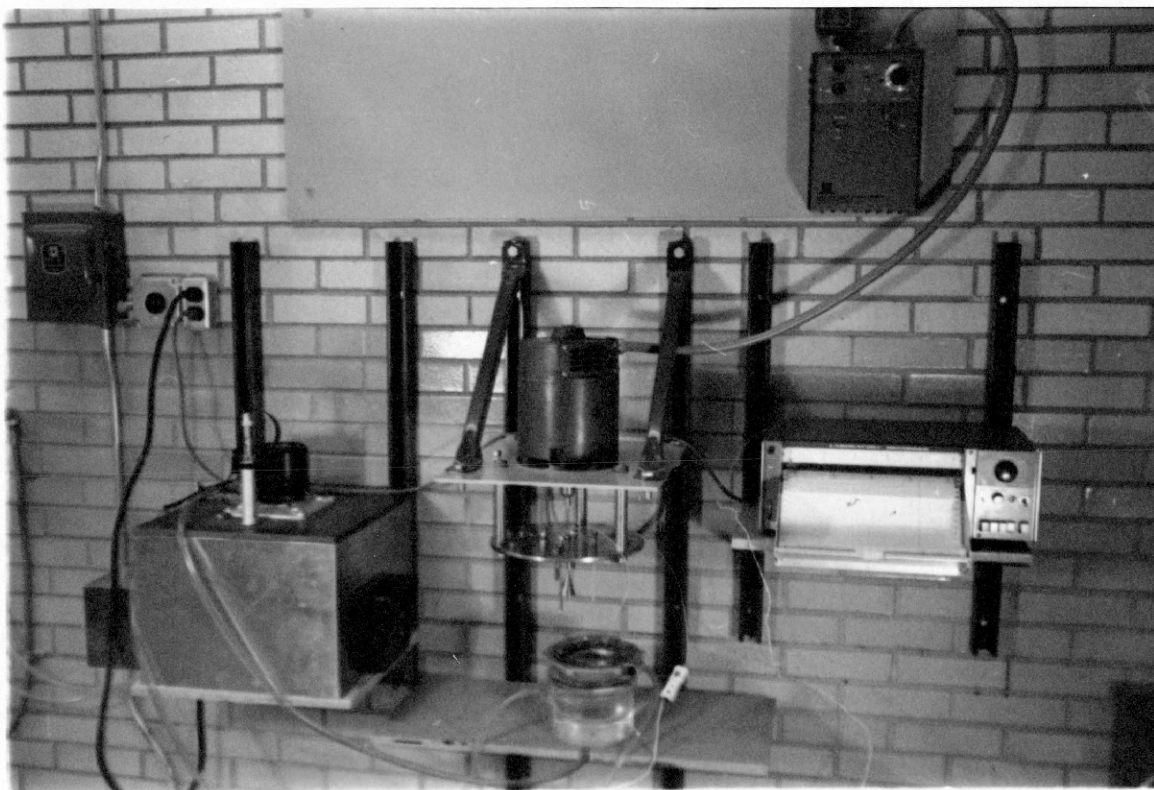
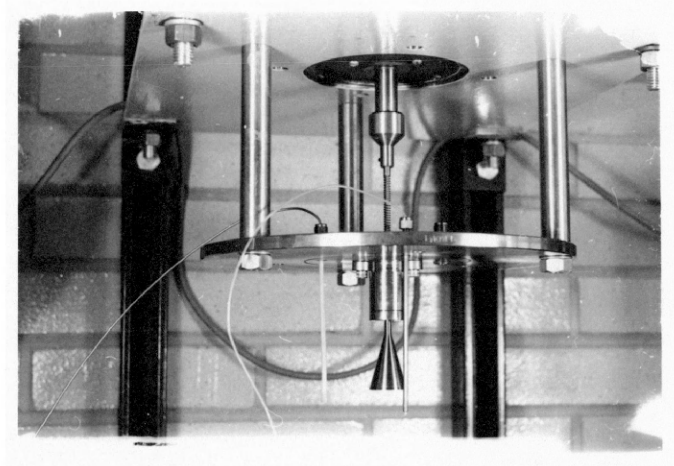
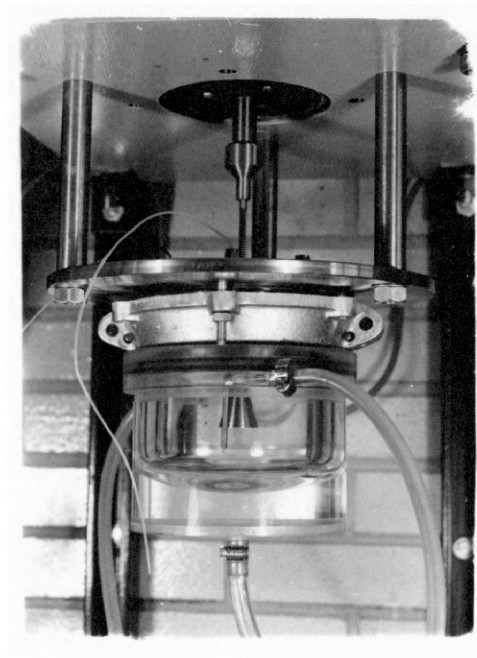


Fig. 4.1. General view of the equipment showing the reactor assembly, temperature bath, recorder and motor speed controller



(a)



(b)

Fig. 4.2. (a) Disk holder set up and (b) Reactor with water jacket mounted in place

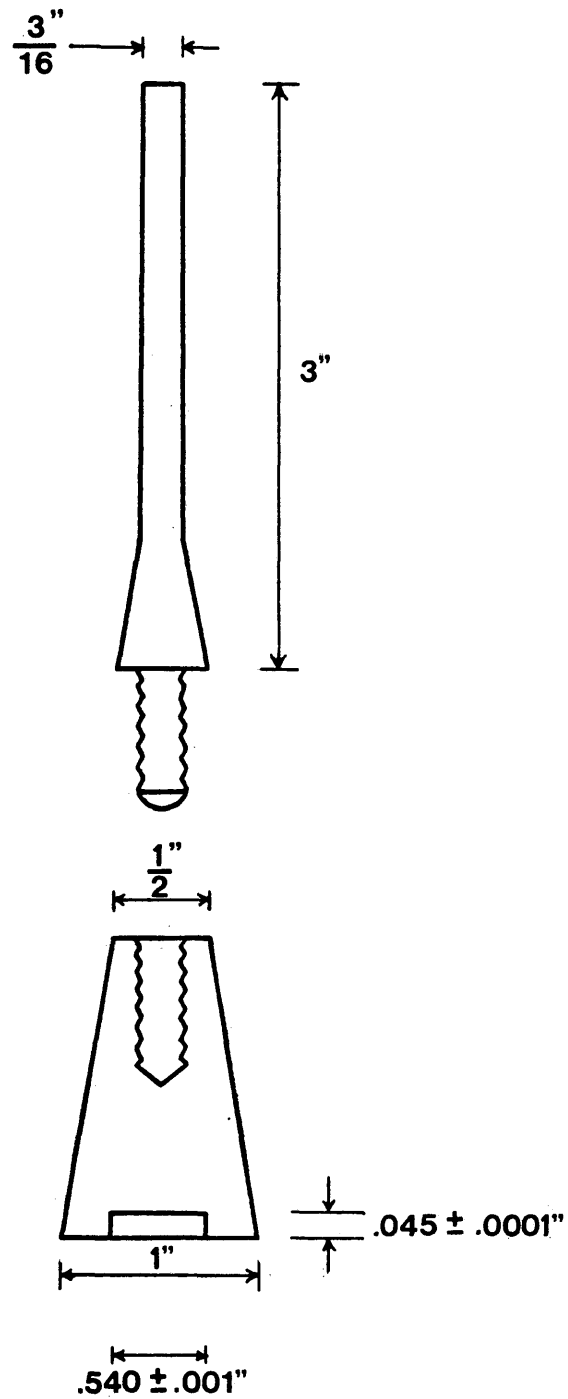


Fig. 4.3. Disk holder sketch showing the two part assembly and the mean dimensions

S

the other of titanium were made. They both consisted of a shaft screwed into a truncated cone as shown in Fig. 4-3. The Cu_2O disks were held in the recess of the conical portion using Loctite 601 sealant.

(c) A water jacket, made of plexiglass, was used to maintain the system at a constant temperature. This jacket was sealed to the pyrex vessel using an O-ring seal. Water from a Model 3052 Lab-Line constant temperature circulating system was circulated in the annular space. The temperature of the system was monitored using a type K (chromel-alumel) thermocouple connected to a Hallmark Data Systems, Type 3043, Strip Chart Recorder. A reference junction of melting ice was also provided.

(d) The speed of rotation was measured by a 1531 model "G.R " Stroboscope.

4.2 Cu_2O Disk Preparation

In order to obtain a polycrystalline Cu_2O sample, pure deoxidized Cu disks, 0.035-in. thick and 0.5-in. diameter, etched with 5m HNO_3 , washed with water and rinsed in acetone, were oxidized. The oxidation was carried out in a Heavy-duty "Multiple Unit" electric furnace at 980°C , using air (total pressure 622 mm Hg), in a recrystallized alumina tube. The furnace was brought to temperature with the disks in a nitrogen atmosphere, to avoid the formation of large amounts of CuO . The samples were completely oxidized in about 16 hours. After this period an additional

six hours for annealing was allowed. A stream of nitrogen was used to flush the tube during cooling to prevent CuO formation. On removal from the furnace the samples showed the presence of a thin layer of CuO, which was removed using abrasive paper down to 4/0. Under these conditions, polycrystalline Cu_2O samples were obtained, averaging 0.10 mm^2 grain area, and 0.525-in. diameter. The method followed in making the Cu_2O is based on the stability diagram Cu/CuO/ Cu_2O system as outlined by G. Honjo(35) .

The temperature required to prevent CuO formation at the oxygen pressure present in the air (160 mm Hg) is $\approx 1030^\circ\text{C}$. However, this temperature could not be obtained in the furnace available.

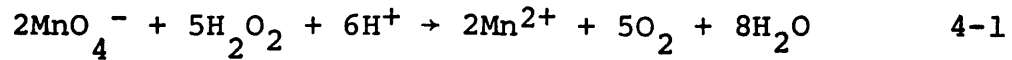
4.3 Reagents Used

- Sulfuric Acid: Dupont reagent grade
- Hydrogen Peroxide: Standard (35%) provided by the Inorganic Chemistry Division of FMC Corporation
- Potassium Permanganate (KMnO_4)-- for the volumetric titration of H_2O_2 : Analytical Grade 99.8% pure
- Sodium Acetate ---to standardize the Potassium Permanganate: Baker's Analyzed Chemical reagent (M.W. 133.99)

4.4 Chemical Analysis

Volumetric analyses were performed in the case of H_2O_2 , using 0.1 N standard solution of Potassium Permanganate, according to the method described by Shumb, Satterfield, and Wentworth (36). The reaction is based on the properties

of the H_2O_2 as a reducing agent, which acts on the MnO_4^- as follows:



The presence of H^+ ions in the reaction is necessary, otherwise the MnO_4^- goes to the formation of colloidal MnO_2 .

Cupric ions in solution was determined using a 306 Perkin-Elmer Atomic Absorption Spectrophotometer. For this purpose standard solutions of 1, 2 and 5 ppm of Cu^{++} were prepared. Three readings, each integrated over two seconds, were averaged to obtain the concentration of a diluted sample.

4.5 Run Procedure

The Cu_2O disk, free of the layer of CuO , was etched in the same solution to be used for the dissolution study, to reveal individual grains. The area of the grains was between $0.093 - 0.112 \text{ mm}^2$. The disk, once etched, washed with distilled water and dried, was mounted in the disk holder using Loctite 601 as sealant. In each run a fresh disk of Cu_2O was used.

The acid solutions were prepared by measuring the amounts of acid and hydrogen peroxide necessary to give the strength required. The reagents were added to a 500 cc volumetric flask containing around 200 cc of distilled water, and then filled to the mark.

The solution was transferred to the unmounted reactor,

and the temperature brought to the desired value. With the disk holder mounted in place and rotating, the speed was measured. The vessel was now raised and fixed to the stainless steel plate, thereby contacting the solution.

During the run, which lasted 60 minutes, 5 ml samples were withdrawn by a syringe at regular intervals. The samples were diluted for Cu^{++} and H_2O_2 Analyses. The runs to study the kinetic mechanism of the dissolution were carried out at 20°C and 800 RPM. To determine the temperature sensitivity, runs at 15, 20, 25 and 30°C were performed. The speed of rotation dependence was studied at 400, 800 and 1600 RPM.

4.6 Visual Observation

The photographs in Fig. 4.4 show the Cu_2O disks before and after dissolution. The sequence (a) shows the polycrystalline structure of the disks at two magnifications. The diameter of the disk was 0.525". In the sequence (b) a partially reacted disk still in the holder is shown on the left. The etched nature of the surface which results in an increase in area may be seen on the right. The surface is shown at high magnification where the diagonal represents the diameter of the disk (0.525"). The effect of this increase in area due to etching is discussed in the chapter 5. ✓

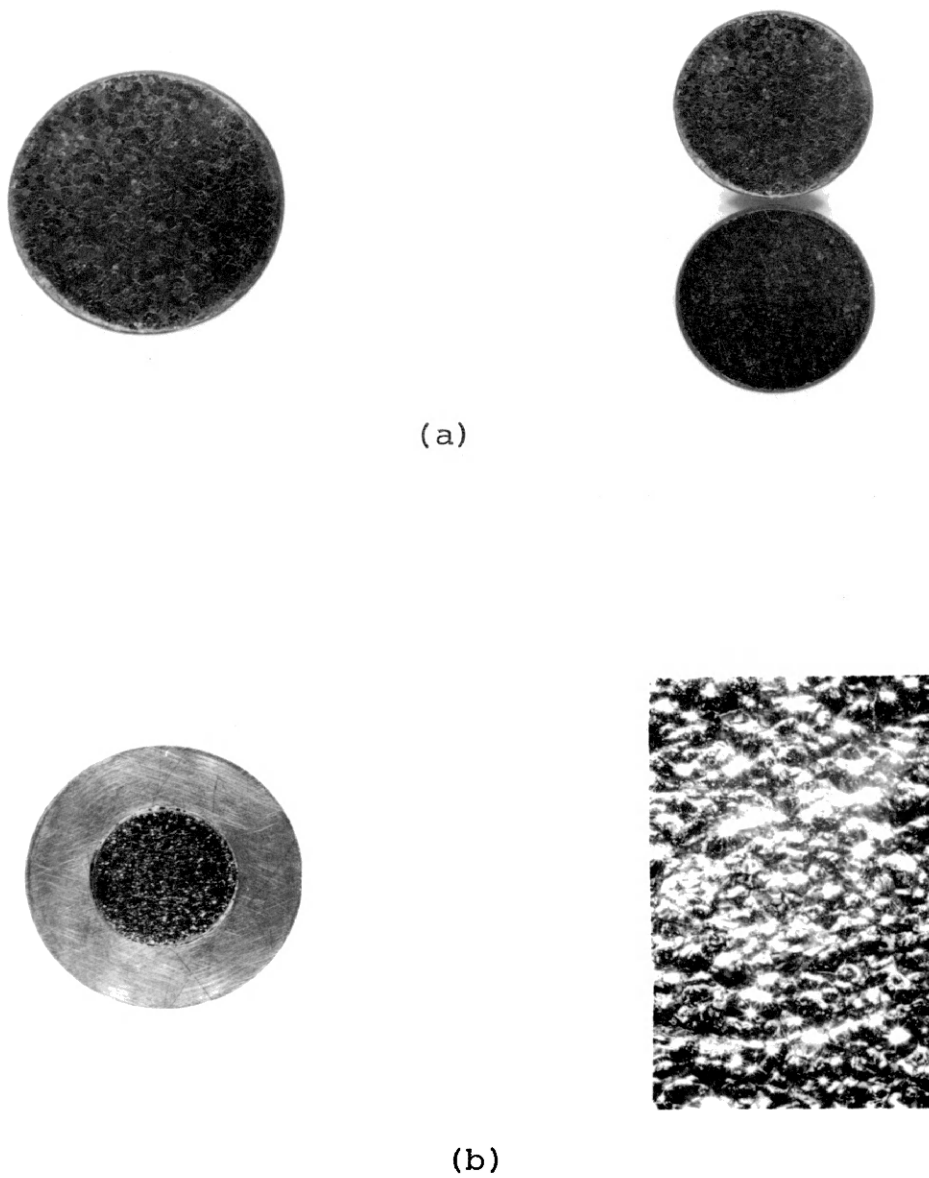


Fig. 4.4 Cu_2O disks before and after dissolution

Chapter 5

RESULTS AND DISCUSSION

In analyzing the experimental data, the following points were taken into consideration:

1. The measured amount of sulphuric acid used was converted to H^+ concentration using the data of Young and Blatz (31), and determined graphically from Fig. 5.1.

2. The characteristic type of behavior obtained by plotting Cu^{++} versus time is shown in Fig. 5.2. Initially, there is an apparent dependence of the overall rate on the Cu^{++} concentration, followed by a zero order reaction. This behavior could be explained by considering that during the initial period, the area subjected to reaction varies until a "steady state" surface structure is obtained, and thereafter the reaction proceeds with uniform area. This was checked by running a prereacted disk, then the initial dependency of the rate on Cu^{++} concentration was not observed. Consequently the data considered for the kinetic analyses of the investigation were taken from the "zero order" region.

The overall dissolution rate for the zero order plots presented in section 1.2 of Appendix 1 was determined from

the slope of the straight line passing through the experimental points and obtained by least squares analysis. The same method was used to fit the data on the Log rate versus $1/T$ from which the activation energy was calculated.

3. The experimental conditions were chosen so that the reaction surface remained free of copper. These conditions were determined from preliminary tests corresponding to minimum concentrations of H_2O_2 of 0.235, 0.353 and 0.471 mol/liter for H_2SO_4 concentrations of 0.40, 0.60, 0.80 mol/liter.

4. The concentration of H_2O_2 was taken as being constant during the runs. This was deduced from the analysis of the H_2O_2 in solution carried out after each run. The method of analysis was capable of discriminating the H_2O_2 concentration to approximately ± 0.1 g/l and typically the analysis yielded changes of the same order of magnitude. It was estimated that at the lowest concentration used the change was less than 2%. It is worth mentioning here also that decomposition of H_2O_2 to oxygen was observed occurring (only) on the surface of the disk as displayed by bubbles of gas nucleating on its surface when the disk was stationary or rotating slowly. However, this loss of H_2O_2 was obviously insignificant based on the remarks made previously.

The same assumption was used for the concentration of $\{H^+\}$ although this was not measured. Stoichiometric calculations revealed that for the lowest concentrations of $\{H^+\}$

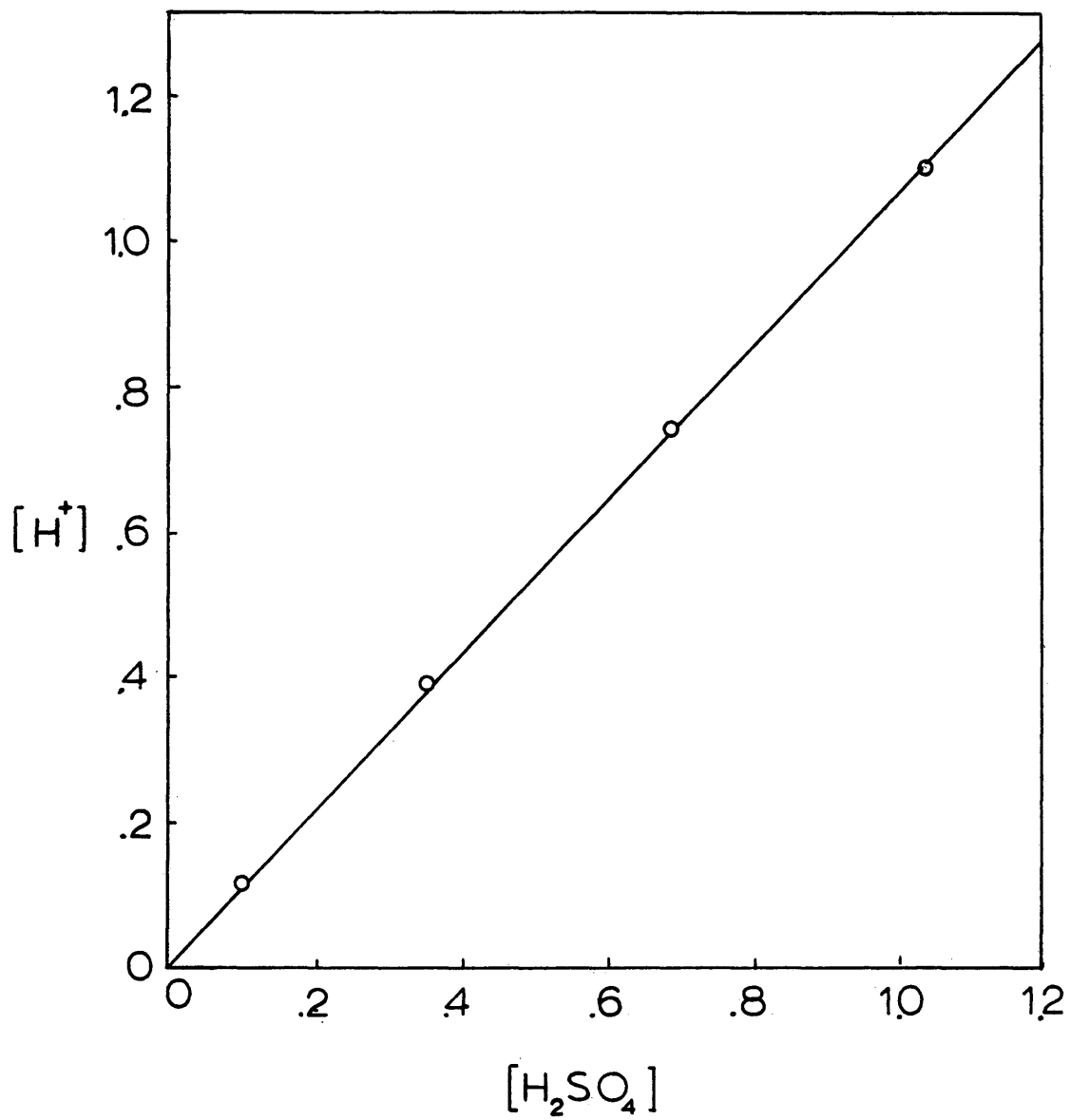


Fig. 5.1. Relation between measured H_2SO_4 and H^+ in solution

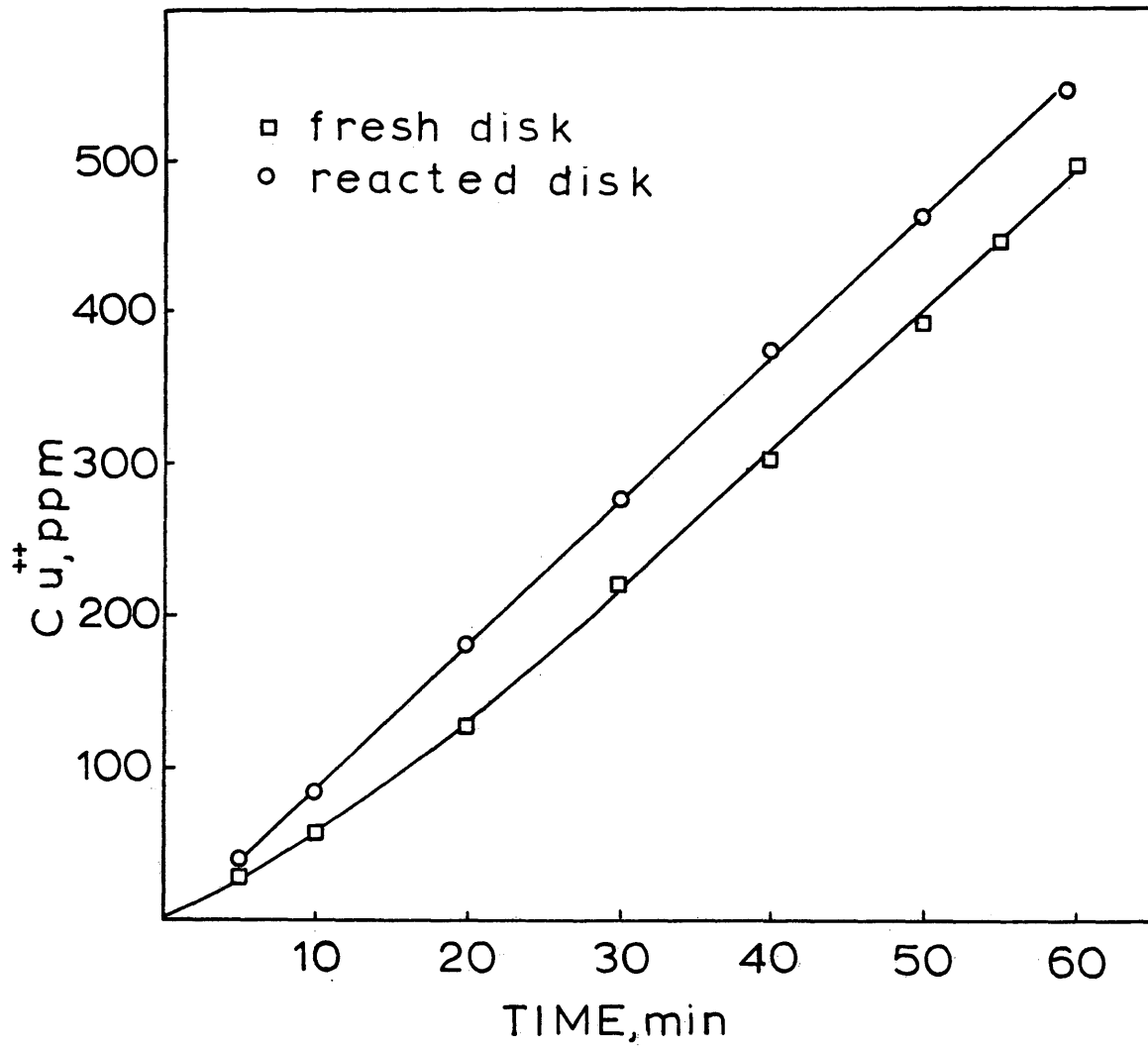


Fig. 5.2. Typical behavior of the Cu_2O dissolution, and complete zero order plot for a reacted disk

used the change was less than 10% of the initial value.

5.1. Analysis of the Parameters

The dissolution kinetics of the Cu_2O in aqueous sulphuric acid solutions with H_2O_2 as oxidant was now studied by determining the effects of the following parameters, and carried out in the order given below:

- (1) Hydrogen ion concentration
- (2) H_2O_2 concentration
- (3) Rotation speed
- (4) Temperature

5.1.1 Hydrogen Ion Concentration

The values of the overall rate for runs 1.1 - 3.10, given in section 1.2 in Appendix 1, were plotted against $\{\text{H}^+\}$ concentration for the three values of H_2O_2 considered, as shown in Fig. 5.3, where the points are the experimental data. It can be seen that the rate experiences an initial rapid increase, followed by a slower increase at higher values of $\{\text{H}^+\}$, with a tendency to level off.

This type of behavior was observed in several investigations (7,34), and corresponds to the type in which the rate is dependent on more than one reactant.

5.1.2 H_2O_2 Concentration

The same type of behavior was observed by plotting the values of the dissolution rate against $\{\text{H}_2\text{O}_2\}$ concentration for the tests 4.1 to 6.7 and shown in Fig. 5.4. This also suggests that in the region studied, the overall rate is controlled by both the H^+ and H_2O_2 concentration.

5.1.3 Rotation Speed

The slopes of the two lines in Fig. 5.5 are practically the same (the values are given in the tables for tests 10.1 and 10.2 included in section 1.2 of Appendix 1), and no dependence on rotation speed can be inferred. From the tests shown in Fig. 5.6 (tests 9.1, 9.2 and 9.3) it can be seen that except for the test at 400 RPM the rate was again essentially constant. The increase in the rate observed for the 400 RPM test is a bit surprising and cannot really be explained. However, it was observed that bubbles appeared on the disk surface at this low RPM and possibly affected the way the surface "etched". Since the presence of these bubbles was also noticeable during preliminary tests at low RPM; all the runs were carried out at 800 RPM to avoid this problem.

5.1.4 Temperature

The temperature sensitivity was investigated in two different regions at 15, 20, 25 and 30°C. The concentration of copper as a function of time for tests 7.1 - 7.4 and 8.1 - 8.4 is tabulated in section 1.1 of Appendix 1. The plots of the tests are shown in Fig. 5.7 and 5.9. The Arrhenius plots for the respective series of tests are shown in Figs. 5.8 and 5.10.

The first series of tests was conducted using 0.471 mol/liter H_2O_2 and 0.860 mol/liter H^+ . The slope from the plot of log rate versus $\frac{1}{T}$ gave an activation energy of 9100 cal/mol

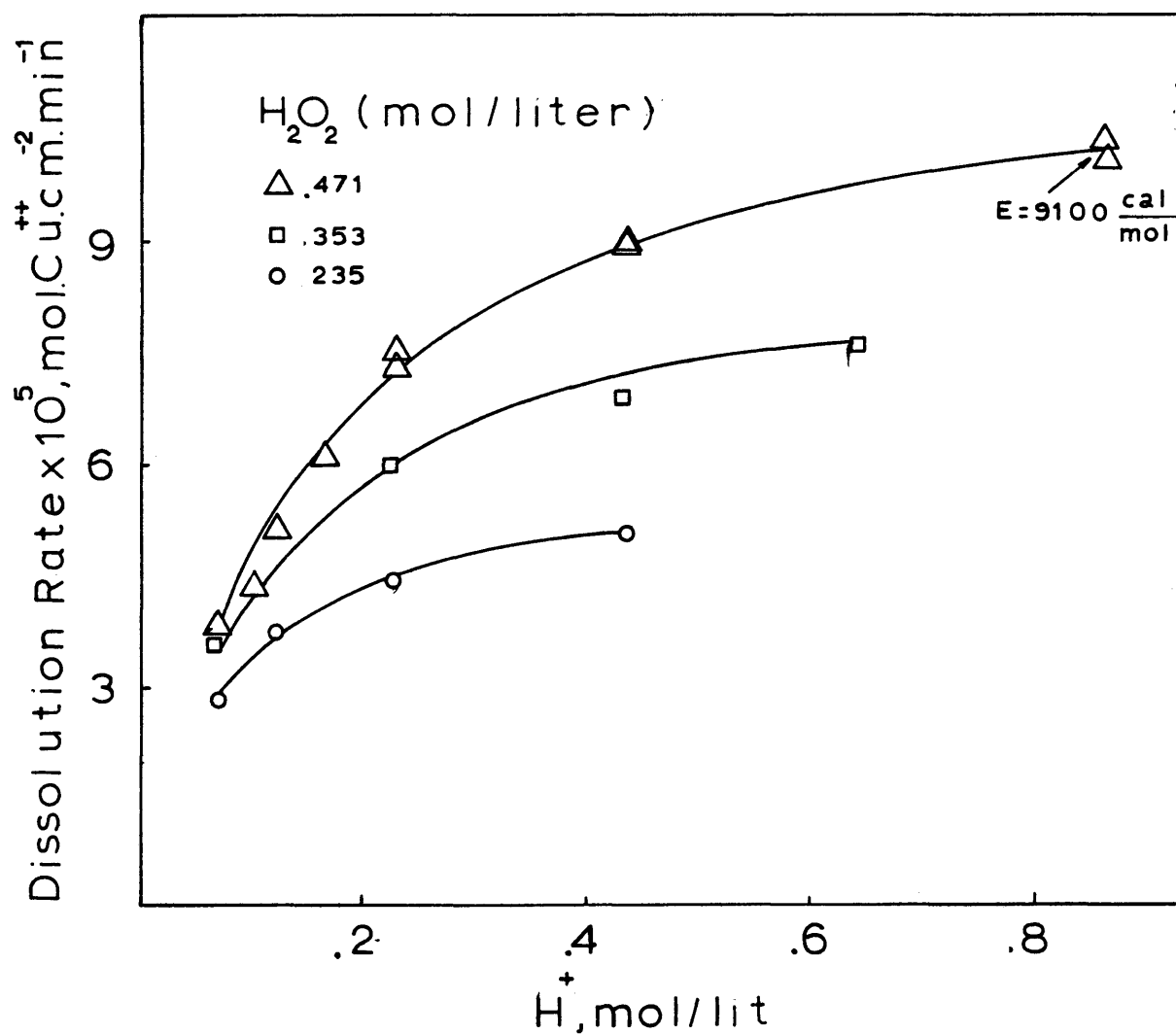


Fig. 5.3. Effect of the $\{\text{H}^+\}$ concentration on the dissolution rate, the continuous lines are the fitted values from the rate equation, and the points represent the experimental data: 20°C , 800 RPM

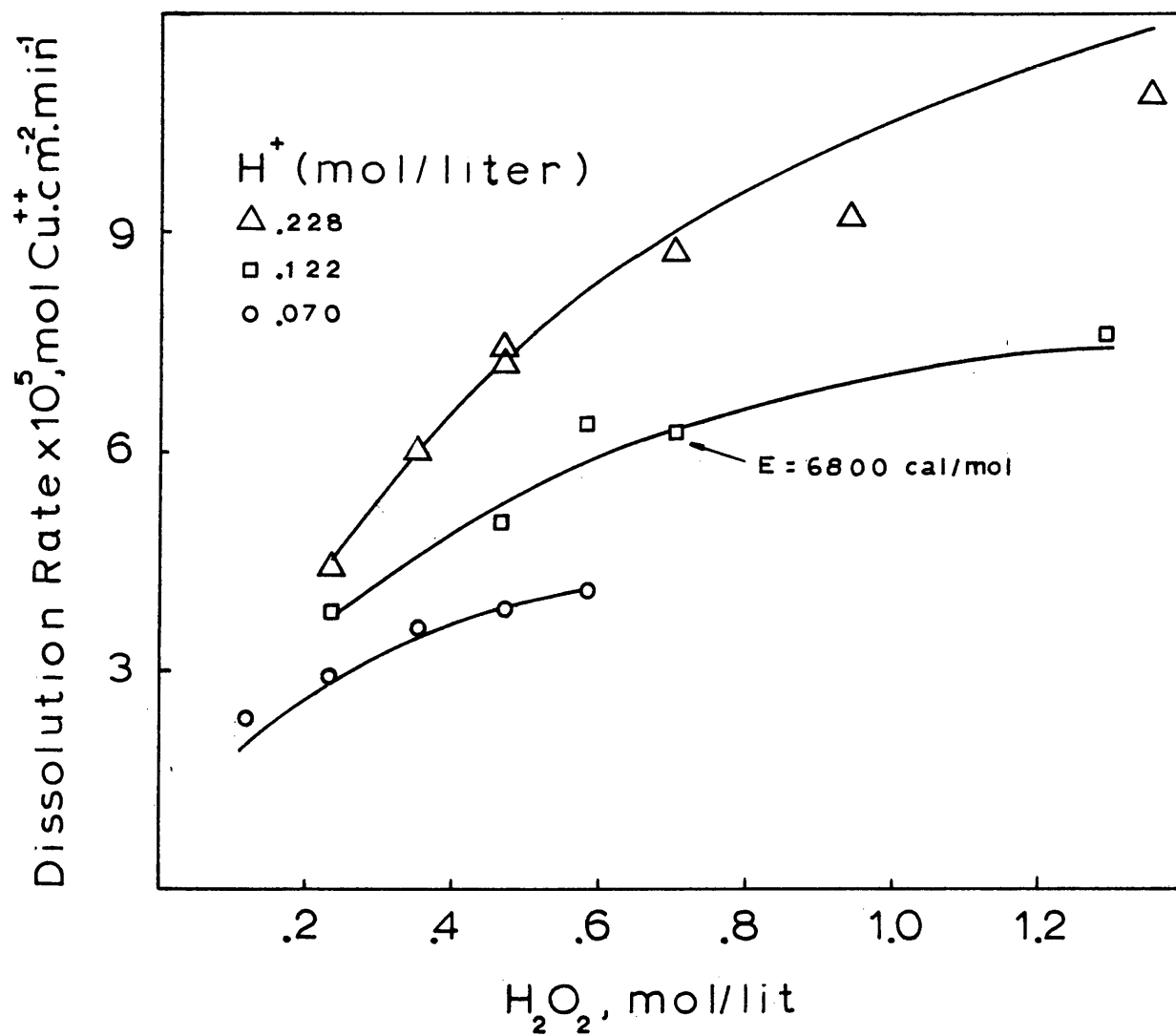


Fig. 5.4. Effect of the H_2O_2 concentration on the dissolution rate. The continuous lines are the predicted value from the rate equation, and the points represent the experimental data: 20°C , 800 RPM.

($E/R = 4,600$ cal). From the second series of tests a lower activation energy of $6,800$ cal/mol ($E/R = 3,422$ cal) was obtained. The conditions in these last tests correspond to $\{H_2O_2\} = 0.706$ mol/liter, $\{H^+\} = 0.122$ mol/liter. Both values obtained seem to indicate chemical controlled processes, and supported the finding on the effects of rotational speed. The lower value at the higher H_2O_2 concentration indicated a possible shift in reaction mechanism and will be discussed subsequently when considering the proposed reaction mechanism.

From the results obtained the following summary may now be given:

(a) The overall rate of the reaction is independent of the concentration of cupric ions (within the range of values present in this investigation -- between 0-700 ppm). However, the rate is dependent on both H_2O_2 and H^+ concentration. In general it would be expected that when the concentration of one reactant is limiting, the overall rate is controlled by the rate associated with this limiting reactant. The behavior observed in all the tests conducted did not seem to indicate that these limiting conditions were achieved.

(b) The tests carried out to determine the effects of speed of rotation and temperature indicated that the overall process was chemically controlled over the range of conditions studied.

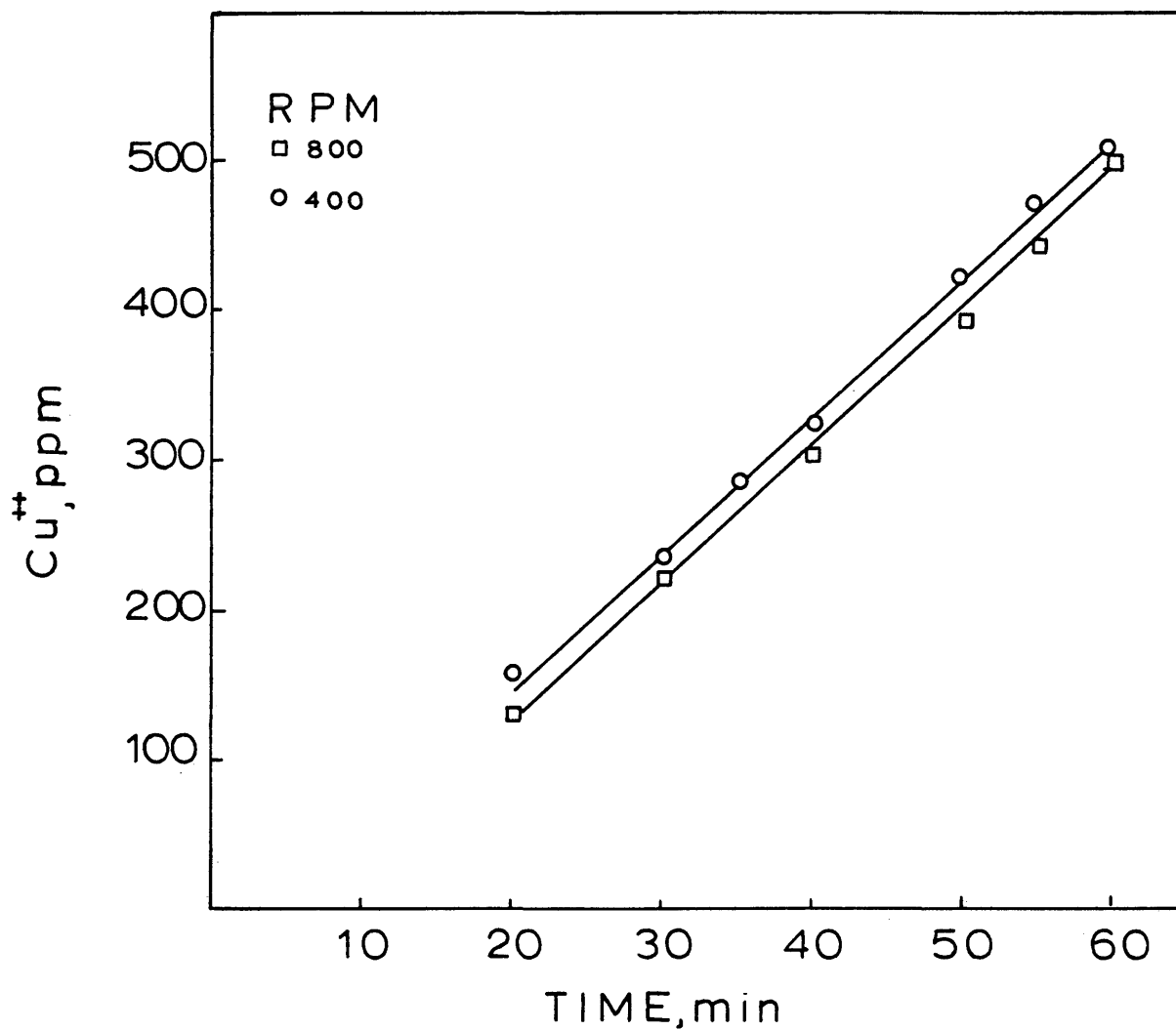


Fig. 5.5. Effect of the speed of rotation on the dissolution of Cu_2O : 0.86 mol/liter H^+ , 0.471 mol/liter H_2O_2 , 20°C

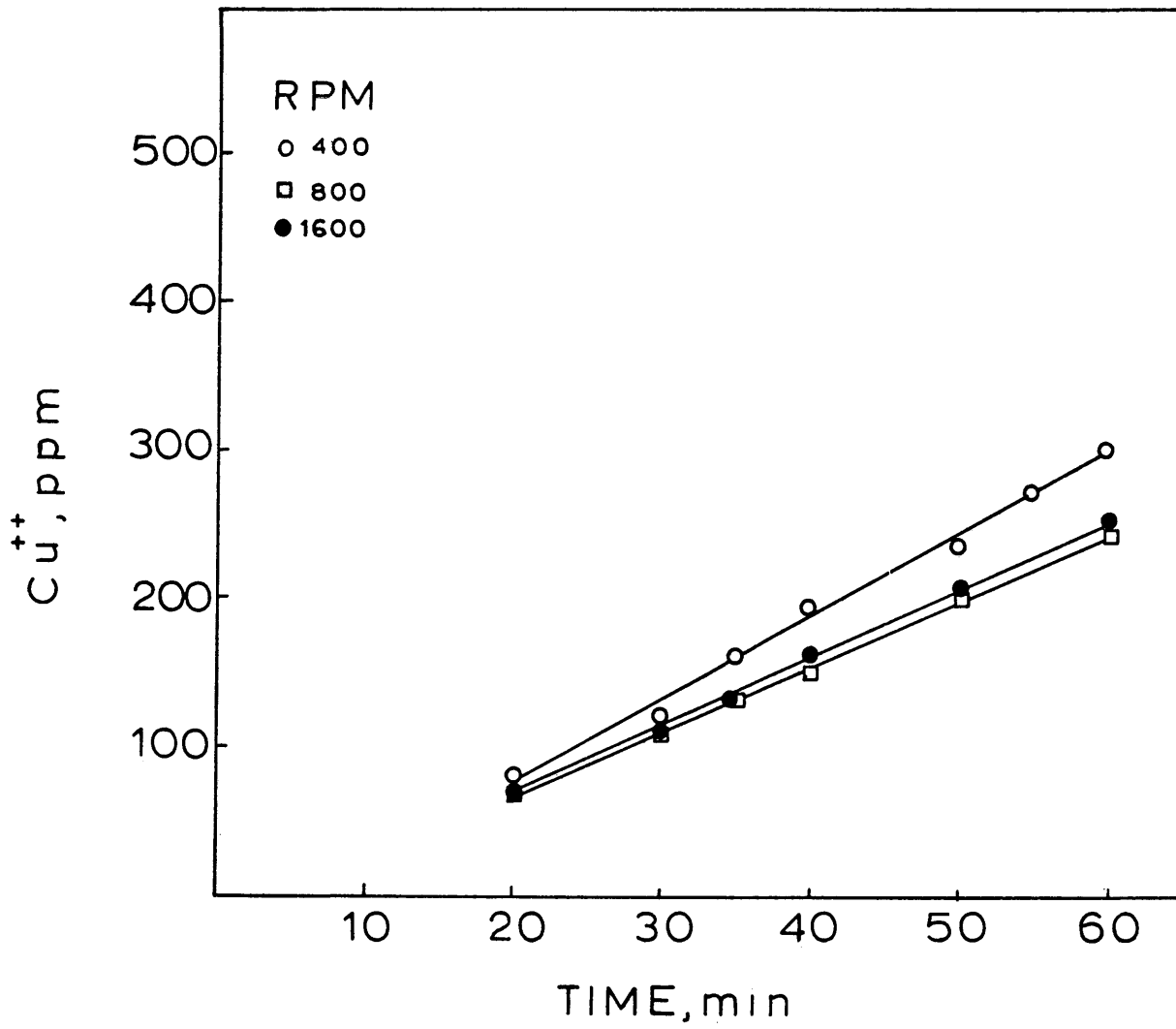


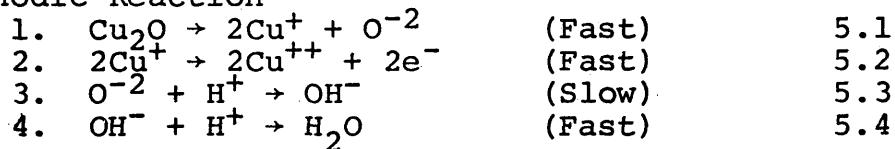
Fig. 5.6 Effect of the speed of rotation on the dissolution of Cu_2O : 0.438 mol/liter H^+ , 0.235 mol/liter H_2O_2 , 20°C

5.2 Proposed Mechanism

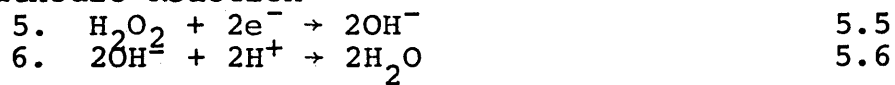
The general rate behavior observed was not unlike that obtained for other dissolution systems, where the reaction mechanism has been developed using an electrochemical approach, such as that given by Habashi (3). The model postulates the presence of local anodic and cathodic areas which account for the dissolution. This approach is particularly well suited to systems which are controlled by the chemical process occurring on the surface of the material under dissolution, as is the case in this study.

The following reactions occurring on the surface of the Cu_2O are proposed.

Anodic Reaction



Cathodic Reaction



Reaction 5.2 is the result of the conditions imposed in this investigation, which inhibited the formation of copper according to the disproportionation reaction:



Reaction 5.4 and 5.6 represent the product OH^- taken away from the surface, the H^+ present will immediately react with the OH^- to form water as dictated by the equilibrium for this reaction.

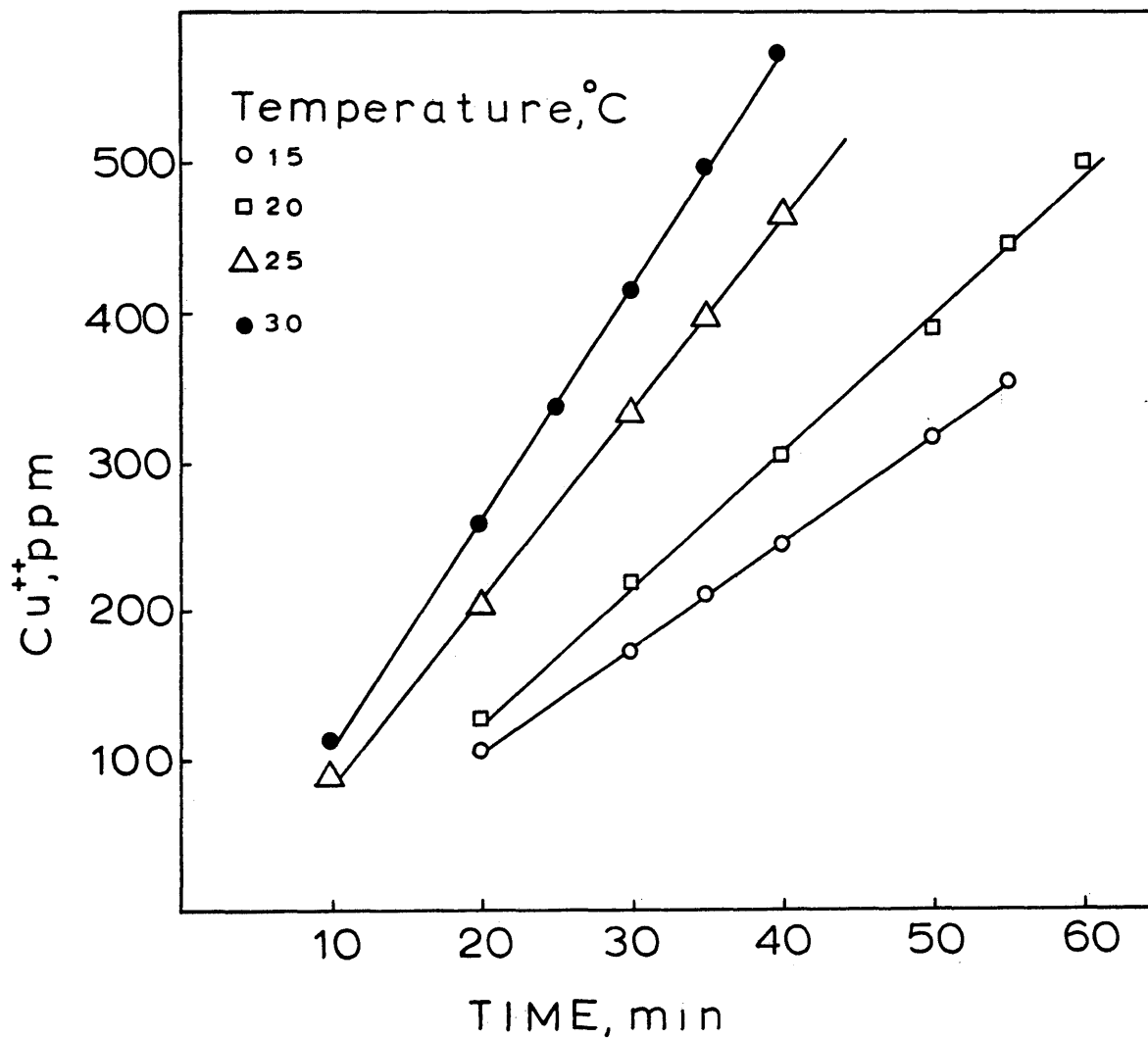


Fig. 5.7. Effect of temperature on the dissolution of Cu_2O :
 $0.86 \text{ mol/liter H}^+$, $0.471 \text{ mol/liter H}_2\text{O}_2$, 800 RPM

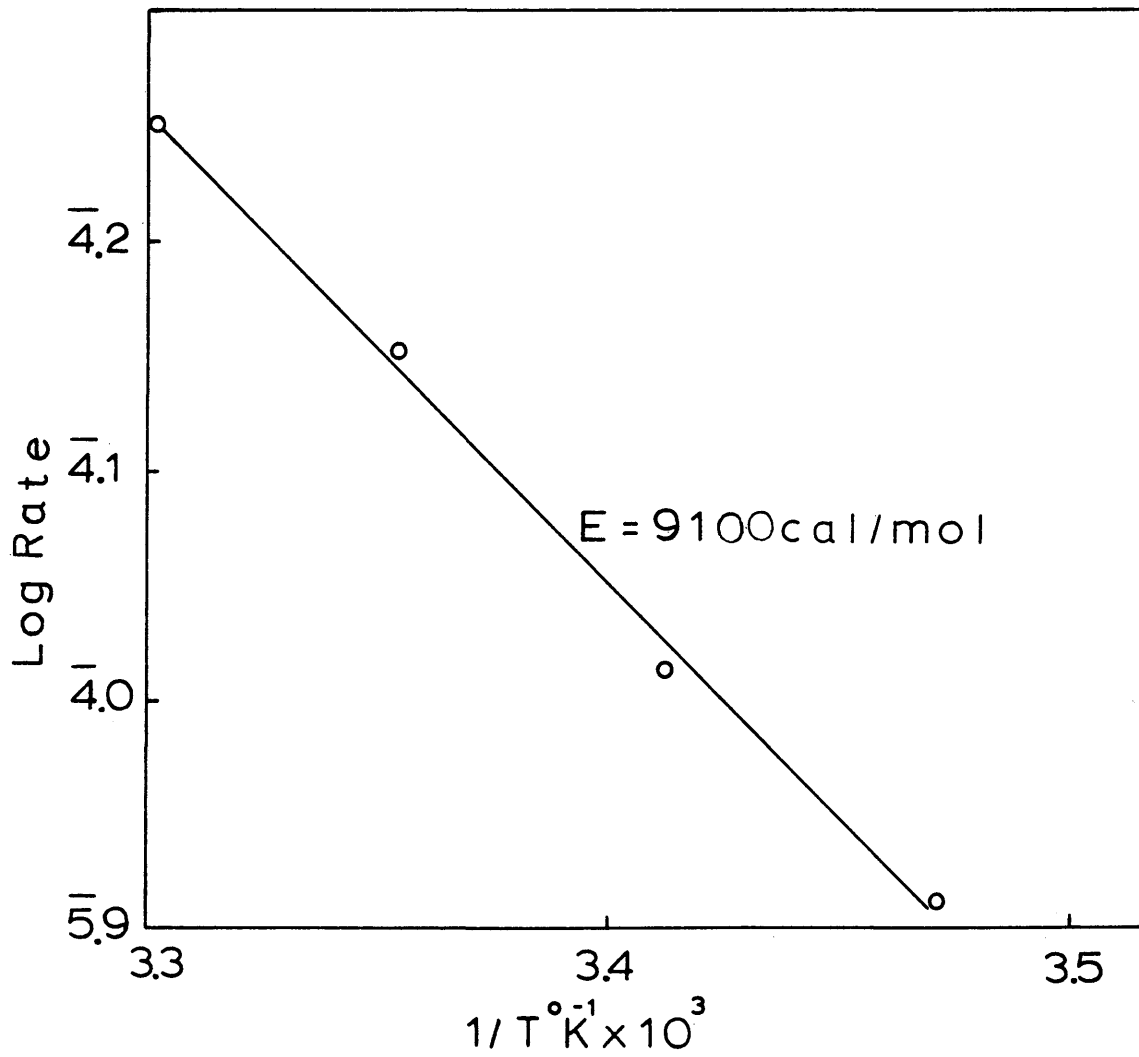


Fig. 5.8. Log rate of reaction vs. reciprocal of temperature for the dissolution of Cu_2O : 0.86 mol/liter H^+ , 0.471 mol/liter H_2O_2 , 800 RPM

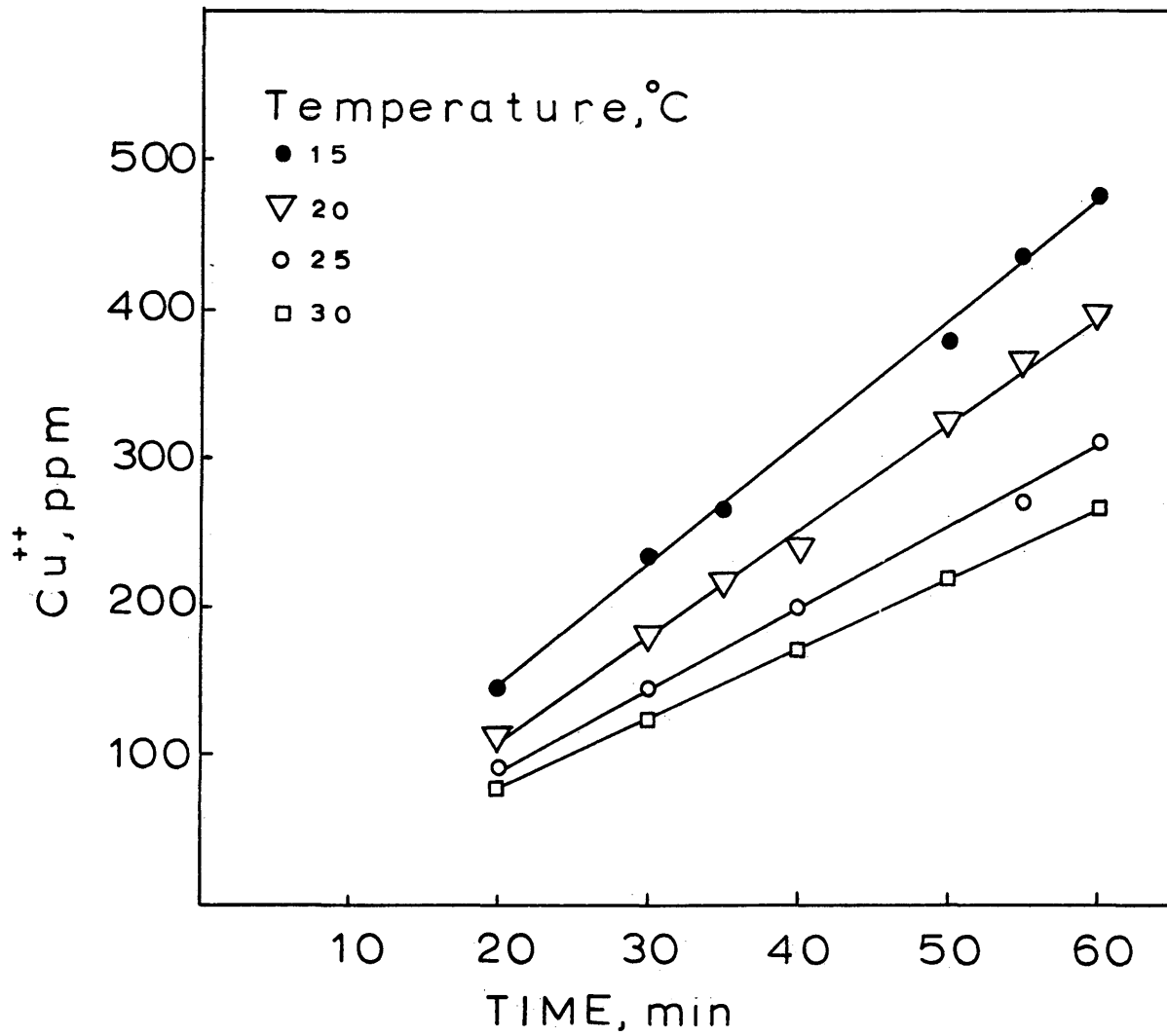


Fig. 5.9. Effect of temperature on the dissolution of Cu_2O : 0.122 mol/liter H^+ , 0.706 mol/liter H_2O_2 , 800 RPM

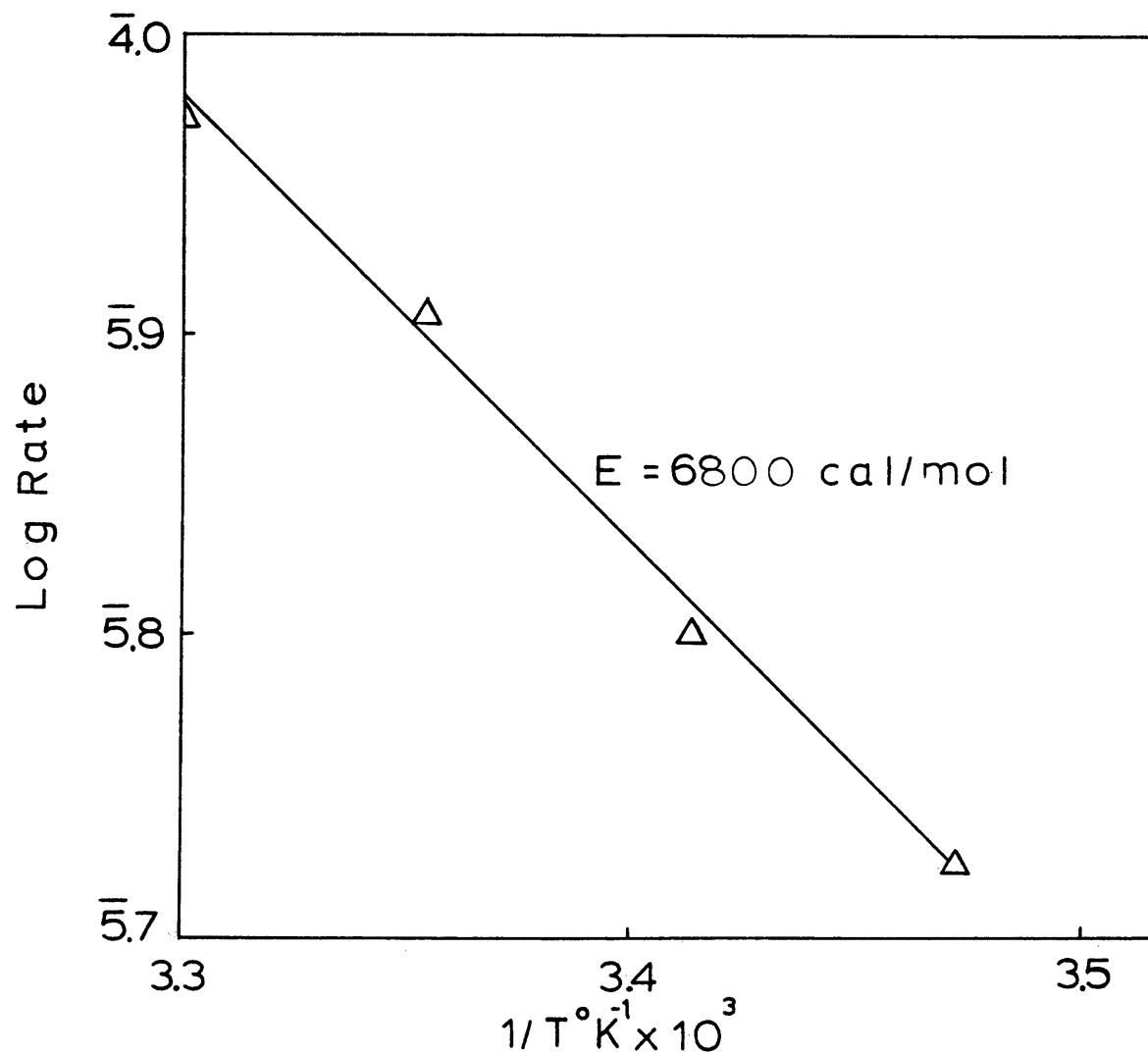


Fig. 5.10. Log rate of reaction vs. reciprocal of temperature for the dissolution of $C_{12}O$: 0.122 mol/liter H^+ 0.706 mol/liter H_2O_2 , 800 RPM

The representation of the anodic and cathodic areas is shown in Fig. 5.11.

Assuming the anodic and cathodic controlled reactions to be elementary, we can consider them first order with respect to $\{H_2O_2\}$ and $\{H^+\}$ respectively, then the anodic and cathodic rate equations will be:

1. Anodic Area (A_1)

$$\text{Rate} = k_1 A_1 \{H^+\} \quad 5.7$$

2. Cathodic Area (A_2)

$$\text{Rate} = k_2 A_2 \{H_2O_2\} \quad 5.8$$

at steady state and considering that

$$A = A_1 + A_2$$

the expression resulting for the specific heterogeneous rate, r'' will be:

$$r'' = \frac{k_1 k_2 \{H^+\} \{H_2O_2\}}{k_1 \{H^+\} + k_2 \{H_2O_2\}} \quad 5.9$$

taking the inverse of this expression:

$$\frac{1}{r''} = \frac{1}{k_2 \{H_2O_2\}} + \frac{1}{k_1 \{H^+\}} \quad 5.10$$

Equation 5.10 is convenient for finding the values of k_1 and k_2 which best fit the data, using a least squares technique. The equations which have to be solved are given in Appendix 2, together with the computer program employed. Values of k_1 and k_2 were obtained using the data from the

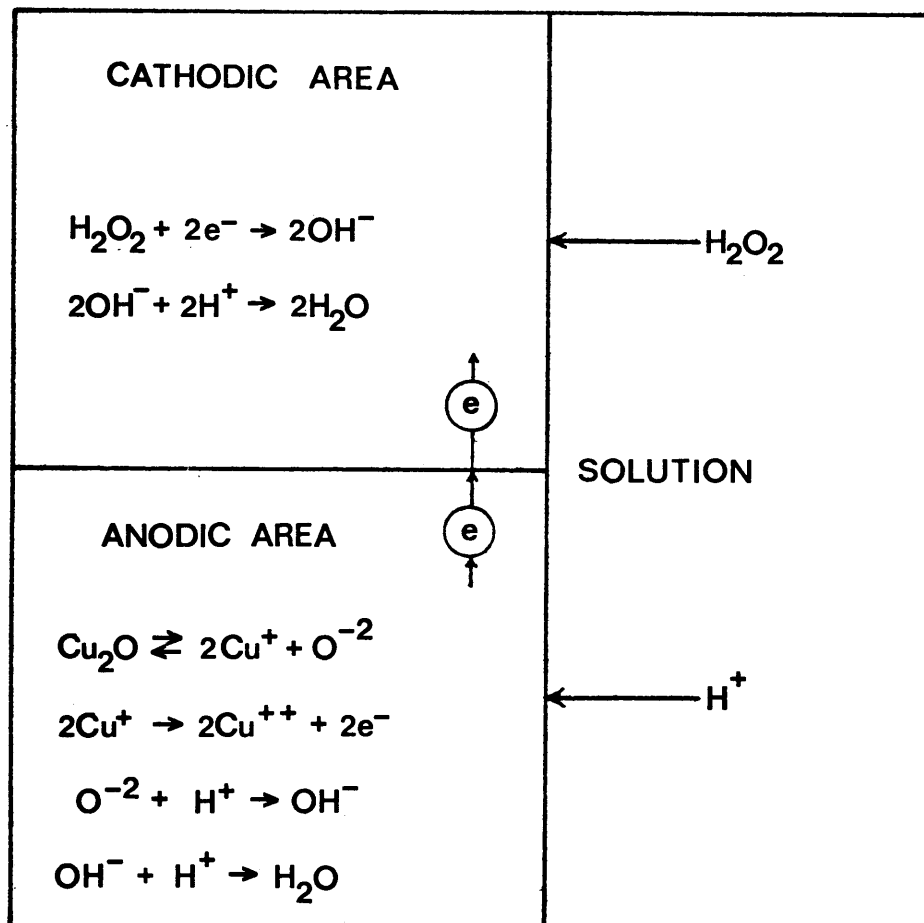


Fig. 5.11. Electrochemical representation of the Cu_2O dissolution (Habashi model)

tests series 1 to 3 tabulated in A.1.2 of Appendix 1.

The values obtained were:

$$k_1 = 7.97 \times 10^{-4} \text{ mol Cu}^{++} \text{ cm}^{-2} \text{ min}^{-1} / \text{mol}\{\text{H}^+\}$$

$$k_2 = 2.53 \times 10^{-4} \text{ mol Cu}^{++} \text{ cm}^{-2} \text{ min}^{-1} / \text{mol}\{\text{H}_2\text{O}_2\}$$

The resulting rate expression is:

$$r'' = \frac{2.02 \times 10^{-7} \{\text{H}^+\}\{\text{H}_2\text{O}_2\}}{7.97 \times 10^{-4} \{\text{H}^+\} + 2.53 \times 10^{-4} \{\text{H}_2\text{O}_2\}}$$

The curve obtained using this expression was drawn as a continuous line in Fig. 5.3. Typical percent deviation of the measured values from this curve was in the order of 5%.

The expression was then used to predict the behavior for the runs shown in Fig. 5.4 (tests series 4 to 6), and as can be seen, reasonable agreement was obtained.

With regard to the activation energy measured and reported in Section 5.1.4 of Chapter 5, it is possible to speculate that the measured values were close to those associated with the cathodic and anodic processes. Thus, the value of 9100 cal/mol, obtained for $\{\text{H}_2\text{O}_2\}$ of 0.471 mol/liter and $\{\text{H}^+\}$ of 0.86 mol/liter, could be assigned to the cathodic process, since the concentration of H_2O_2 becomes limiting under those conditions. Similarly the value of 6800 cal/mol, obtained for $\{\text{H}_2\text{O}_2\}$ of 0.706 mol/liter and

$\{H^+\}$ of 0.122 mol/liter, could be assigned to the anodic process, since the concentration of H^+ now becomes limiting. The points in the $\{H_2O_2\}$, $\{H^+\}$ region, in which the measurements were made is shown in Fig. 5.3 and 5.4 respectively.

It should, however, be realized that limitations on the extent to which one or other of the reactants could be increased did not allow a definitive statement on this point to be made. In particular, for a given H_2O_2 concentration the H^+ concentration cannot be increased beyond a value which makes the ratio of $\{H_2O_2\}/\{H^+\} < 0.54$ since copper will be obtained on the surface. Also, for a given H^+ concentration, if $\{H_2O_2\}$ is increased to too large a value, its decomposition occurs.

Chapter 6

CONCLUSION

The conclusions deduced from the results of this study are presented in this final chapter, together with suggestions for future work.

6.1 Summary of Conclusions

The conclusions deduced from the present investigation of the dissolution of Cu_2O in acidic solutions of $\text{H}_2\text{SO}_4 - \text{H}_2\text{O}_2$ are as follows:

1. The presence of Cu^{++} plays no role in the Cu_2O dissolution, at least in the range of concentration studied (0 - 500 ppm).
2. The dissolution rate was found to be independent of the speed of rotation above 400 RPM. Thus, the process is controlled only by chemical reactions on the surface of the Cu_2O . This was confirmed by the values of the activation energies (9100 and 6800 cal/mol) determined.
3. The conditions under which this investigation was carried out, did not result in the formation of copper on the surface. The conditions involve H_2O_2 concentrations of 0.118-1.353 mol/liter and H^+ concentrations of 0.07-0.86 mol/liter (0.05-0.80 mol/liter H^+). This corresponds to a $\{\text{H}_2\text{O}_2\}/\{\text{H}^+\}$ ratio greater than 0.54 at 20°C . In addition

under these conditions the anodic and cathodic reactions occurring appear to be equally important, and the limiting behavior where only one of them becomes important was not encountered.

4. The rate expression for the dissolution of Cu_2O in $\text{H}_2\text{SO}_4\text{-H}_2\text{O}_2$ solutions at 20°C , under the conditions tested was found to be:

$$\begin{aligned} \text{DISSOLUTION RATE } \{ \text{mol Cu}^{++} \text{ cm}^{-2} \text{ min}^{-1} \} \\ = \frac{2.02 \times 10^{-7} \{ \text{H}_2\text{O}_2 \} \{ \text{H}^+ \}}{7.91 \times 10^{-4} \{ \text{H}^+ \} + 2.53 \times 10^{-4} \{ \text{H}_2\text{O}_2 \}} \end{aligned}$$

from a practical point of view the rate expression predicts a scale Cu_2O removal rate in the order of $12 \text{ micron} \cdot \text{min}^{-1}$ at $0.86 \text{ mol/liter H}_2\text{SO}_4$ and $0.471 \text{ mol/liter H}_2\text{O}_2$. This is equivalent to dissolving a 1 mm thick disk in less than one hour, which was in fact observed in the runs carried out.

6.2 Future Work

There are two obvious questions to which answers can be given, only after further work. These are:

(a) What is the effect of Cu^{++} concentration on the dissolution of Cu_2O (Cu^{++} concentrations greater than 0.5 g/l)?

(b) What is the effect of Cu^{++} concentration on the H_2O_2 decomposition?

Since the range of Cu^{++} concentration of interest could be as high as 30 g/l there are certain experimental consid-

erations which should be noted. At these high concentrations, significant changes in concentration have to be obtained in order for the results to be accurate. This requires the use of either a large disk -- to increase the rate of dissolution -- or small volume of solution; the latter condition not being very practical.

With regard to the homogeneous catalyzed decomposition of H_2O_2 by Cu^{++} , it is probably best to study this independently.

APPENDIX I

Test Results for the Dissolution of Cuprite (Cu_2O) in
Sulphuric Acid and Hydrogen Peroxide Solutions

A.1.1 Tables of Copper Concentration as a Function of Time for the Dissolution Tests

Table 1.1

H_2O_2 : 0.235 mol/liter T: 20^oC RPM: 800 AREA: 1.4 cm²

Test No.	1.1	1.2	1.3	1.4
H^+ mol/l	0.070	0.122	0.228	0.438
Time (minutes)	Cu^{++} (ppm)			
5	8.7	16.3	24.8	15.7
10	27.2	24.2	26.8	31.6
20	37.3	50.6	58.9	66.5
30	63.2	77.6	95.7	109.3
35	-	93.8	113.9	132.3
40	88.7	120.0	133.0	150.5
50	113.0	156.4	168.6	200.7
55	130.5	168.5	192.3	-
60	140.3	184.3	220.0	244.6

Table 1.2

H₂O₂: 0.353 mol/liter T: 20°C RPM: 800 AREA: 1.4 cm²

Test No.	2.1	2.2	2.3	2.4
H ⁺ mol/l	0.070	0.228	0.438	0.649
Time (minutes)	Cu ⁺⁺ (ppm)			
5	12.1	21.7	21.2	23.3
10	24.3	41.2	40.2	44.1
20	48.7	87.8	88.0	98.5
30	77.8	141.0	141.3	154.7
35	93.6	165.0	172.3	187.3
40	108.8	190.7	202.0	218.0
50	137.3	247.6	265.8	285.7
55	164.2	272.8	300.8	329.4
60	174.0	301.2	326.5	366.3

Table 1.3

H₂O₂: 0.471 mol/liter T: 20°C RPM: 800 AREA: 1.4 cm²

Test No.	H ⁺ mol/l									
	3.1	3.2	3.3	3.4	3.5	3.6	3.7	3.8	3.9	3.10
	0.070	0.102	0.122	0.165	0.228	0.228	0.438	0.438	0.860	0.860
Time (minutes)	Cu ⁺⁺ (ppm)									
5	-	12.5	16.8	18.6	24.8	24.6	24.6	25.5	26.5	28.4
10	34.0	24.0	31.3	35.5	43.2	46.9	51.6	53.6	55.5	60.0
20	62.1	51.7	68.8	78.8	111.7	105.3	116.0	114.1	127.5	135.3
25	-	-	-	-	-	-	-	-	-	174.5
30	101.1	87.3	107.0	130.3	177.0	162.0	184.8	188.2	219.0	218.0
35	118.0	103.2	128.3	134.7	198.8	199.5	224.3	229.2	-	255.0
40	128.0	115.9	147.0	184.5	233.0	235.0	268.7	269.3	300.3	306.0
45	-	-	-	-	-	-	-	-	-	355.7
50	174.0	162.0	193.3	237.5	305.3	299.1	350.7	-	387.5	404.3
55	-	183.5	226.0	258.6	330.3	-	393.7	-	442.1	-
60	196.5	199.6	243.0	293.6	367.7	-	430.8	432.1	499.2	-

Table 1.4

H^+ : 0.070 mol/liter T: 20°C RPM: 800 AREA: 1.4 cm²

Test No.	4.1	4.2	4.3	4.4	4.5
H_2O_2 mol/l	0.118	0.235	0.353	0.471	0.588
Time (minutes)	Cu^{++} (ppm)				
5	8.8	8.7	12.1	-	23.5
10	16.7	27.2	24.3	34.0	39.5
20	33.8	37.3	48.7	62.1	55.0
30	57.9	63.2	77.8	101.1	93.2
35	-	-	93.6	118.0	108.8
40	81.3	88.7	108.8	128.0	127.2
50	96.0	113.0	137.3	174.0	165.7
55	-	130.5	164.2	-	179.3
60	119.3	140.3	174.0	196.5	199.8

Table 1.5

H^+ : 0.122 mol/liter T: 20°C RPM: 800 AREA: 1.4 cm²

Test No.	5.1	5.2	5.3	5.4	5.5
H_2O_2 mol/l	0.235	0.471	0.588	0.706	1.294
Time (minutes)	Cu^{++} (ppm)				
5	16.3	16.8	28.3	22.8	28.4
10	24.2	31.3	46.3	40.6	51.7
20	50.6	68.8	-	90.8	110.8
30	77.6	107.0	153.8	144.2	180.5
35	93.8	128.3	174.6	182.3	214.5
40	120.0	147.0	206.5	200.0	248.8
50	156.4	193.3	266.6	-	312.0
55	168.5	226.0	288.6	271.0	348.0
60	184.3	243.0	322.5	313.0	382.2

Table 1.6

H⁺: 0.228 mol/liter T: 20°C RPM: 800 AREA: 1.4 cm²

Test No.	6.1	6.2	6.3	6.4	6.5	6.6	6.7
H ₂ O ₂ mol/l	0.235	0.353	0.471	0.471	0.706	0.941	1.353
Time (minutes)	Cu ⁺⁺ (ppm)						
5	24.8	21.7	24.8	24.6	24.8	27.9	43.7
10	26.8	41.2	43.2	46.9	52.8	54.5	77.4
20	58.9	87.8	111.7	105.3	118.4	118.2	167.5
30	95.7	141.0	177.0	162.0	191.0	193.7	255.0
35	113.9	165.0	198.8	199.5	222.6	229.8	323.0
40	133.0	190.7	233.0	235.5	267.3	283.5	372.6
50	168.6	247.6	305.3	299.1	336.3	350.8	463.0
55	192.3	272.8	330.3	-	387.8	395.0	506.6
60	220.0	301.2	367.7	-	422.2	454.1	-

Table 1.7

H_2O_2 : 0.471 mol/liter H^+ : 0.860 mol/liter

RPM: 800 AREA: 1.4 cm^2

Test No. 7.1 7.2 7.3 7.4

Time (minutes)	T (°C)	15	20	25	30
		Cu ⁺⁺ (ppm)			
5		-	26.5	43.1	54.9
10		48.6	55.5	88.8	114.0
20		107.2	127.5	204.0	259.7
25		-	-	-	336.7
30		173.7	219.0	330.3	415.5
35		212.5	-	394.0	497.5
40		243.5	300.3	465.8	572.1
50		316.9	387.5	-	-
55		353.8	442.1	-	-
60		400.8	499.2	-	-

Table 1.8

H_2O_2 : 0.706 mol/liter H^+ : 0.122 mol/liter

RPM: 800 AREA: 1.4 cm^2

Test No.	8.1	8.2	8.3	8.4
T (°C)	15	20	25	30
Time (minutes)	Cu ⁺⁺ (ppm)			
5	-	22.8	24.8	32.8
10	38.2	40.6	46.9	67.3
20	78.6	90.8	112.0	145.3
25	120.6	144.2	180.0	234.7
30	-	-	215.4	263.0
40	169.3	200.0	248.7	-
50	218.3	-	324.2	378.0
55	244.5	271.0	362.7	436.8
60	263.0	313.0	396.3	475.0

Table 1.9

H_2O_2 : 0.235 mol/liter H^+ : 0.438 mol/liter
 T: 20°C AREA: 1.4 cm²

Test No.	9.1	9.2	9.3
SPEED (RPM)	400	800	1600
Time (minutes)	Cu ⁺⁺ (ppm)		
5	21.2	15.7	-
10	37.6	31.6	40.7
20	82.9	66.5	71.7
30	123.3	109.3	112.5
35	164.0	132.3	131.7
40	194.7	150.5	164.3
50	238.0	200.7	209.0
55	275.7	-	232.7
60	306.3	244.6	256.5

Table 1.10

H_2O_2 : 0.471 mol/liter H^+ : 0.860

T: 20°C AREA: 1.4 cm²

Test No.	10.1	10.2
SPEED (RPM)	400	800
Time (minutes)	Cu ⁺⁺ (ppm)	
5	20.2	26.5
10	54.2	55.5
20	155.7	127.5
30	231.3	219.0
35	282.3	-
40	320.7	300.3
50	422.7	387.5
55	471.7	442.1
60	504.0	499.2

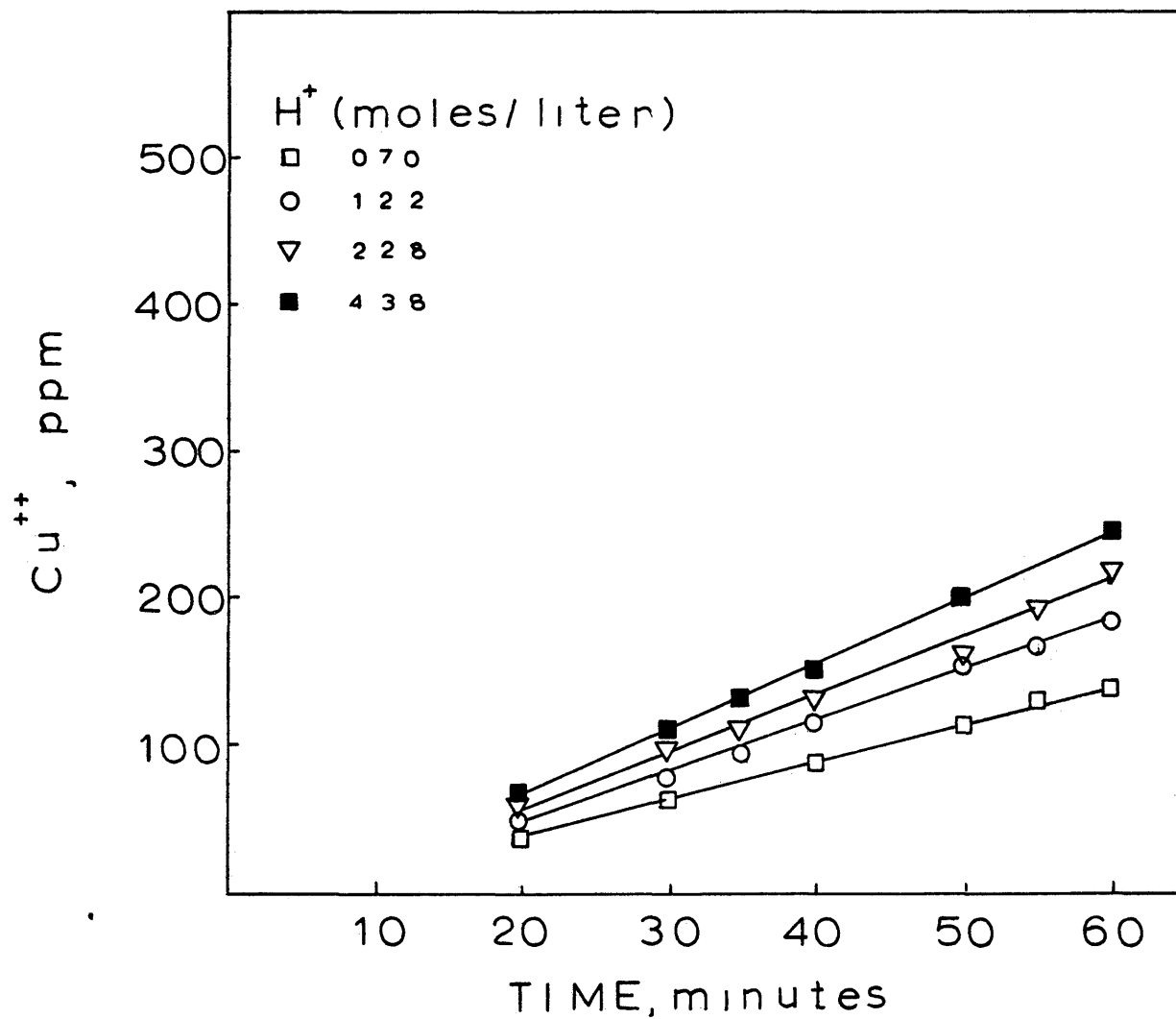


Fig. A.1.1 Dissolution of Cu_2O in 0.235 mol/liter of H_2O_2 at different H^+ concentrations: 20°C, 800 RPM

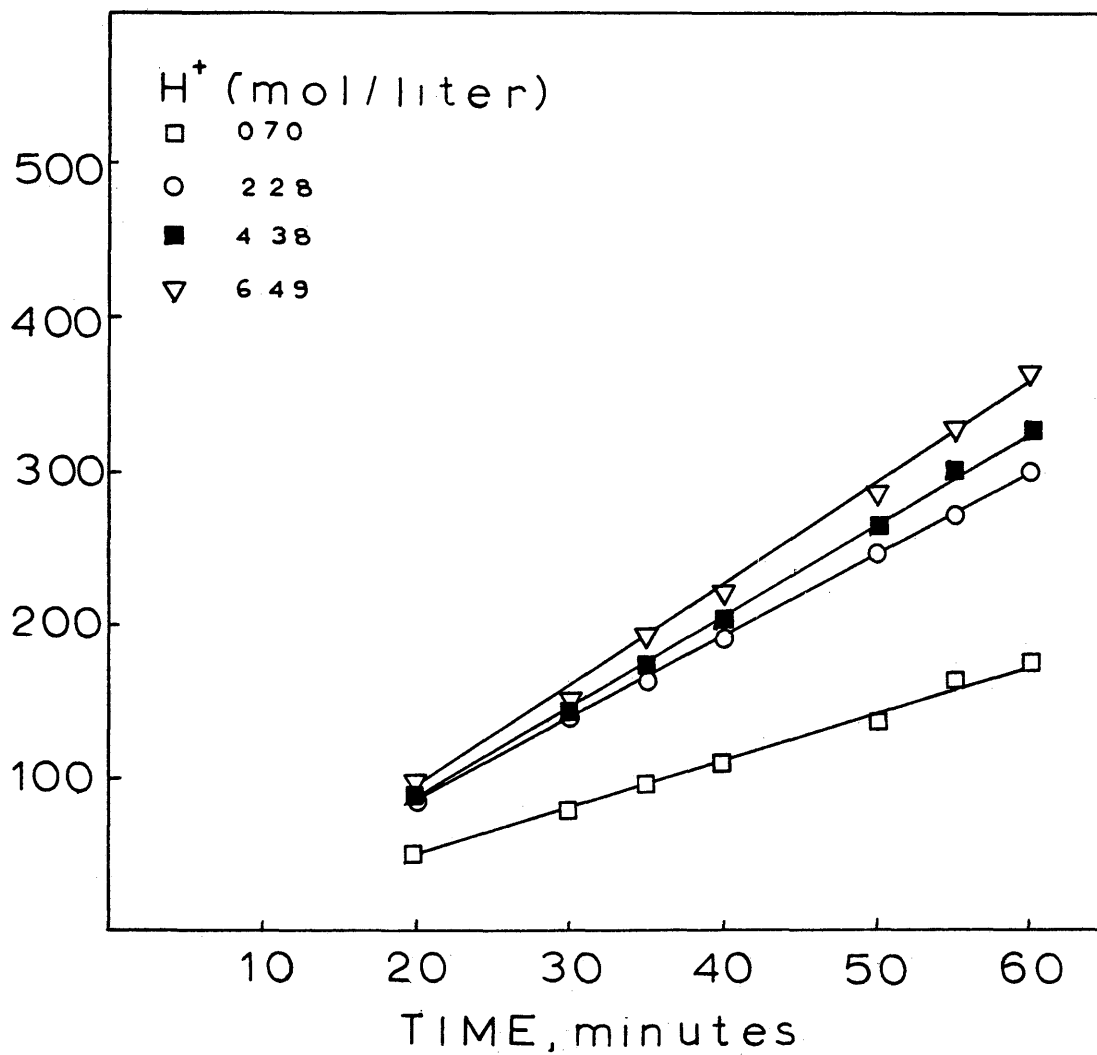


Fig. A.1.2 Dissolution of Cu_2O in 0.353 mol/liter H_2O_2 at different H^+ concentrations: $20^\circ C$, 800 RPM

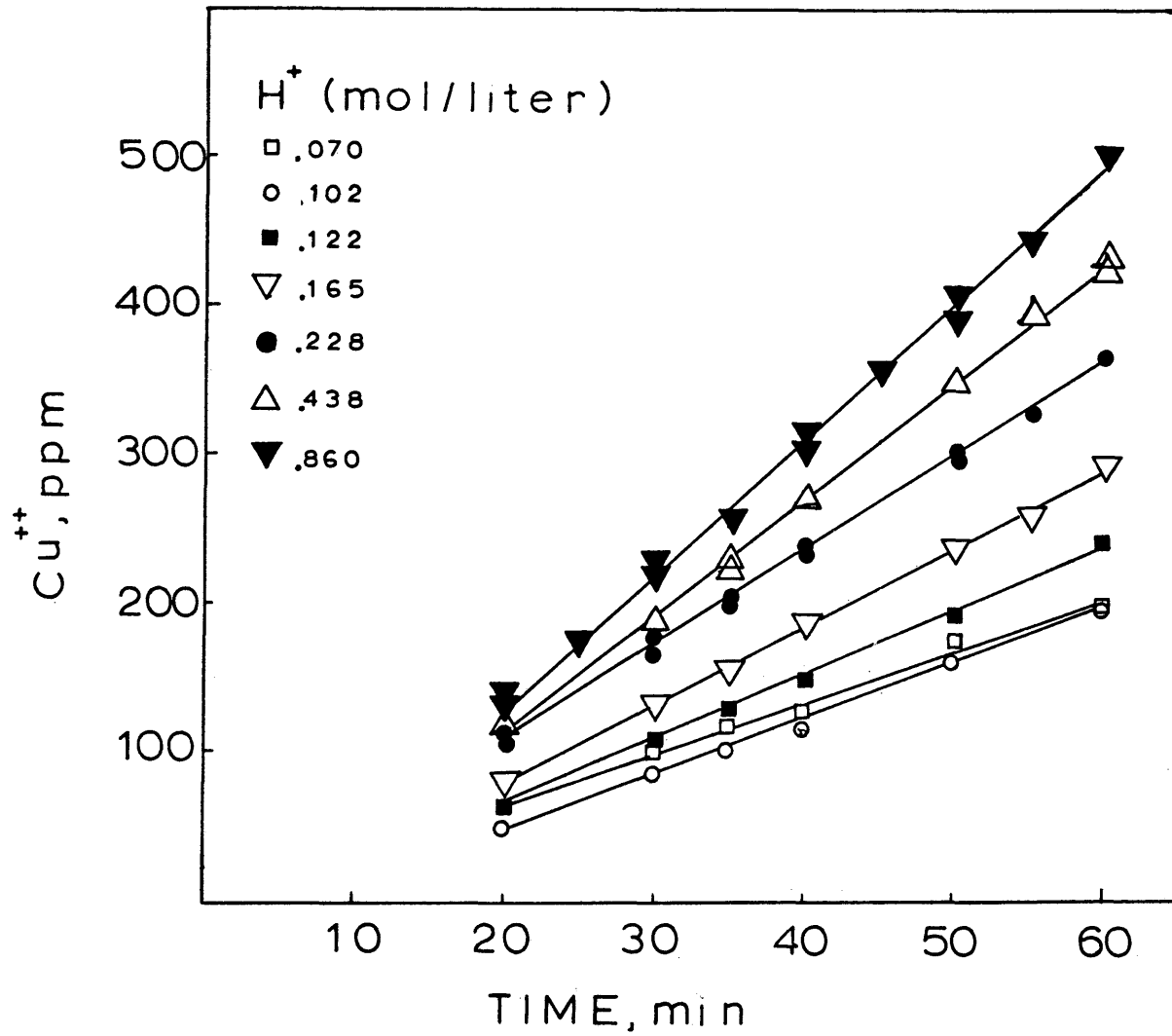


Fig. A.1.3 Dissolution of Cu_2O in 0.471 mol/liter H_2O_2 , at different H^+ concentrations : 20°C, 800 RPM

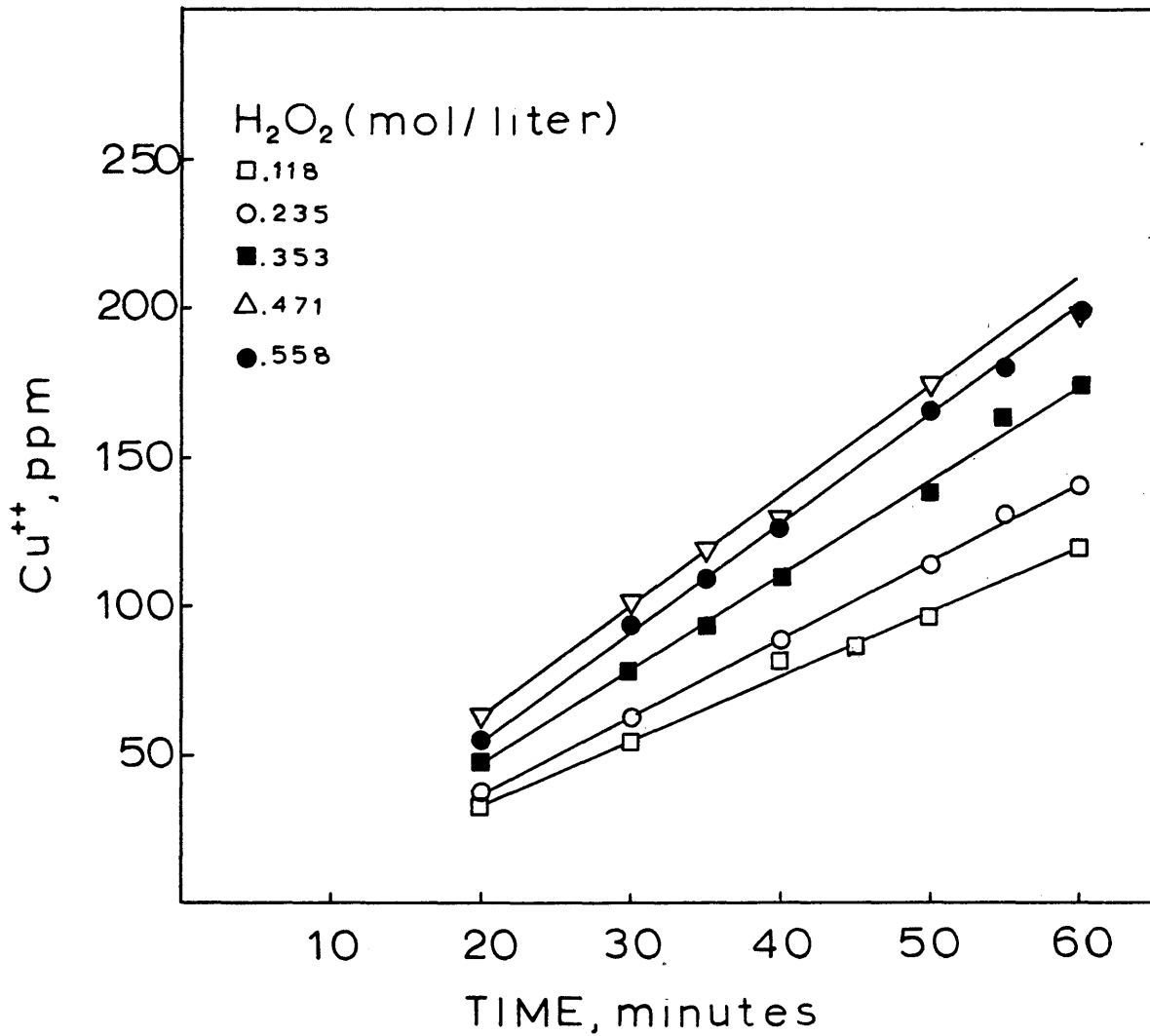


Fig. A.1.4 Dissolution of Cu_2O in 0.07 mol/liter H^+ at different concentrations of H_2O_2 : 20°C, 800 RPM

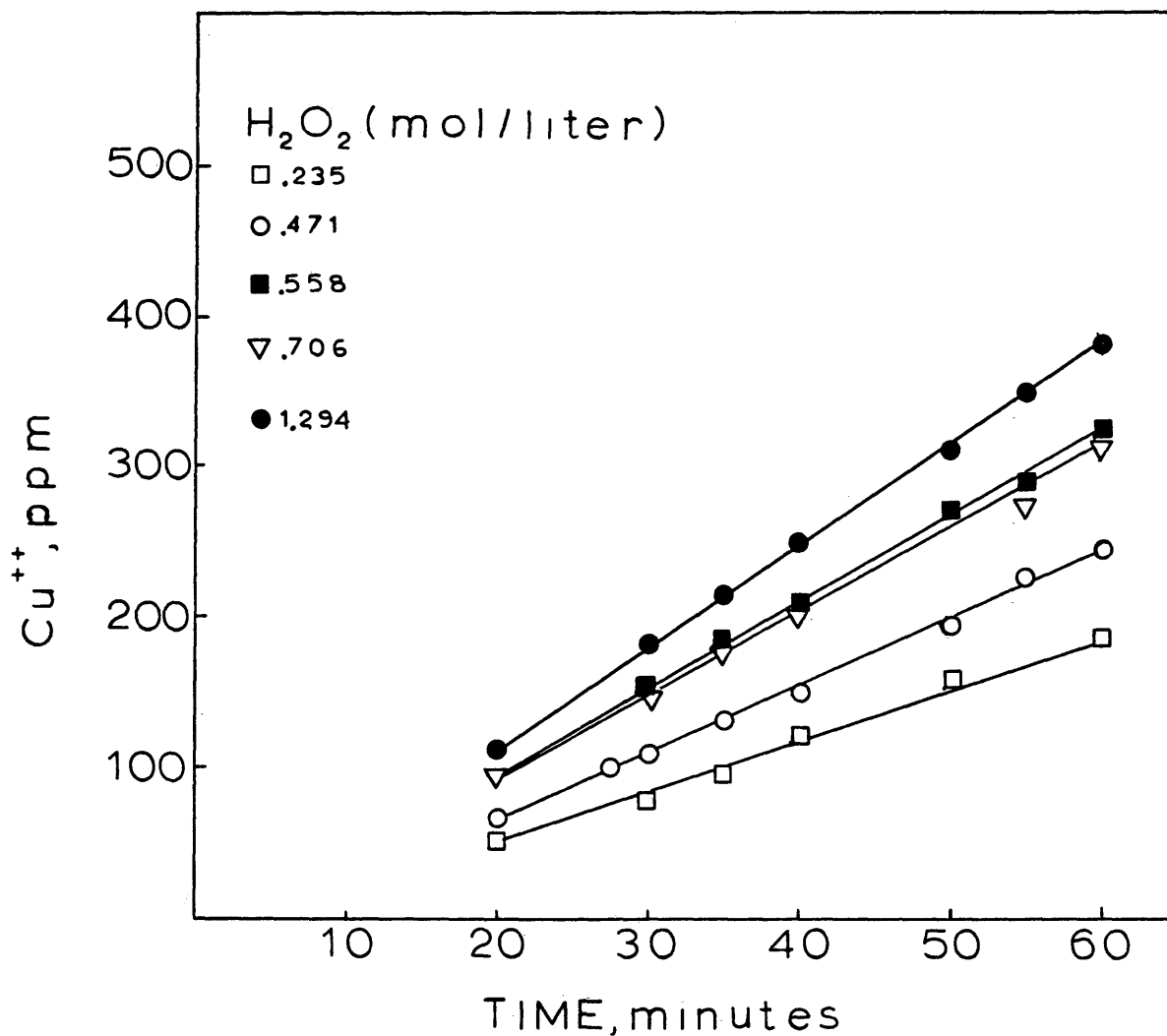


Fig. A.1.5 Dissolution of Cu_2O in 0.122 mol/liter H^+ at different concentrations of H_2O_2 : 20°C, 800 RPM.

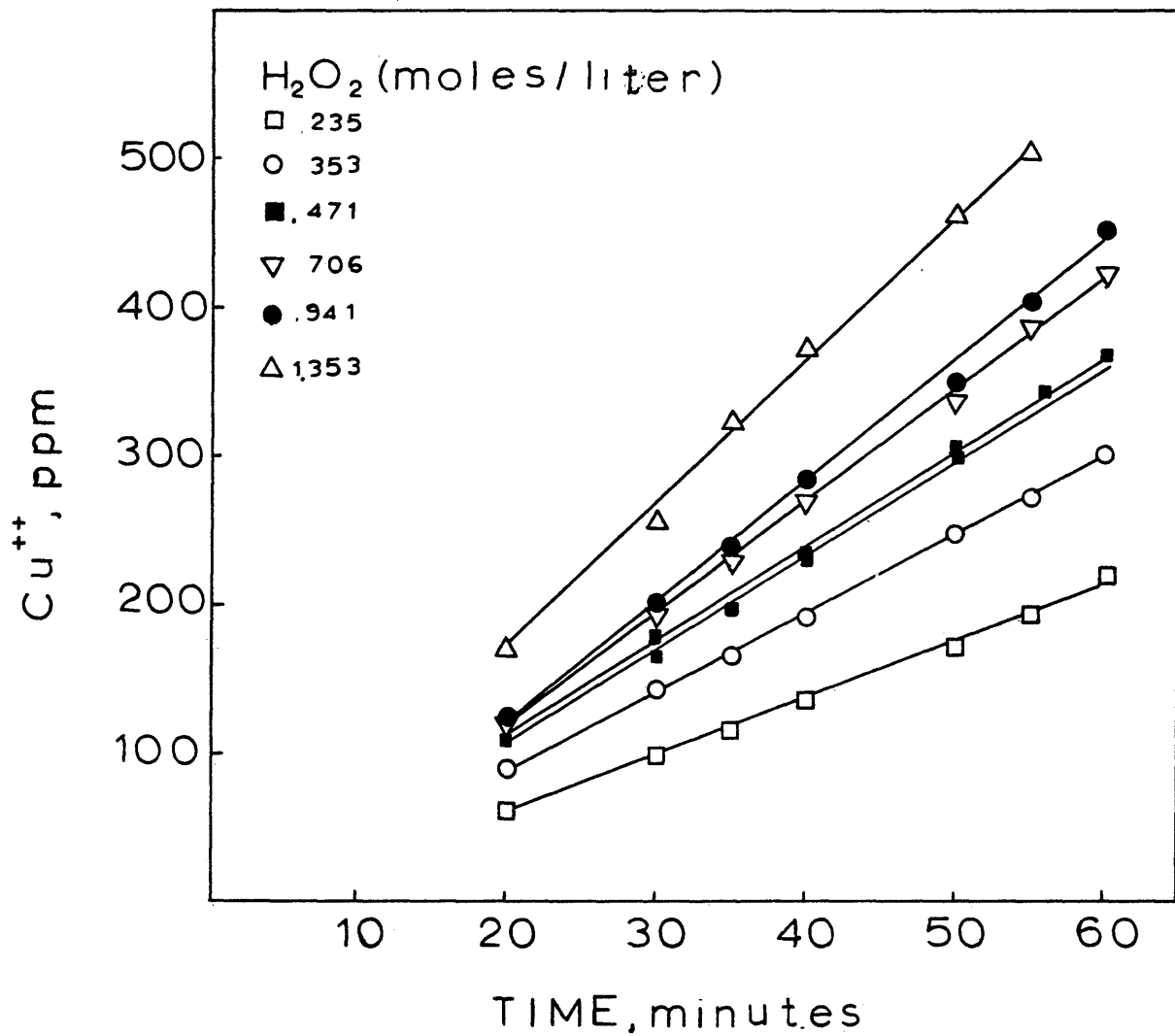


Fig. A.1.6 Dissolution of Cu_2O in 0.228 mol/liter H^+ at different concentrations of H_2O_2 : 20°C, 800 RPM

Appendix A.1.2 Summary of the Overall Dissolution Rate Values

Test No.	Dissolution Rate (ppm Cu ⁺⁺ min ⁻¹)	Dissolution Rate x 10 ⁵ (mol Cu ⁺⁺ cm ⁻² min ⁻¹)
1.1	2.59	2.92
1.2	3.37	3.79
1.3	3.93	4.43
1.4	4.47	5.04
2.1	3.19	3.59
2.2	5.33	6.01
2.3	6.09	6.86
2.4	6.73	7.59
3.1	3.40	3.83
3.2	3.76	4.24
3.3	4.45	5.02
3.4	5.31	5.98
3.5	6.39	7.21
3.6	6.54	7.37
3.7	8.03	9.05
3.8	7.98	8.99
3.9	9.10	10.26
3.10	8.98	10.12
4.1	2.08	2.34
4.2	2.59	2.92
4.3	3.19	3.59
4.4	3.40	3.83
4.5	3.59	4.02

Appendix A.1.2 (continued)

Test No.	Dissolution Rate (ppm Cu ⁺⁺ min ⁻¹)	Dissolution Rate x 10 ⁵ (mol Cu ⁺⁺ cm ⁻² min ⁻¹)
5.1	3.37	3.79
5.2	4.45	5.02
5.3	5.67	6.39
5.4	5.56	6.26
5.5	6.73	7.58
6.1	3.93	4.43
6.2	5.33	6.01
6.3	6.39	7.21
6.4	6.54	7.37
6.5	7.65	8.62
6.6	8.23	9.27
6.7	9.64	10.86
7.1	7.25	8.16
7.2	9.10	10.26
7.3	12.54	14.16
7.4	15.71	17.70
8.1	4.71	5.31
8.2	5.56	6.27
8.3	7.17	8.08
8.4	8.32	9.38
9.1	5.62	6.34
9.2	4.45	5.02

Appendix A.1.2 (continued)

Test No.	Dissolution Rate (ppm Cu ⁺⁺ min ⁻¹)	Dissolution Rate x 10 ⁵ (mol Cu ⁺⁺ cm ⁻² min ⁻¹)
9.3	4.70	5.30
10.1	9.00	10.15
10.2	9.10	10.26

APPENDIX II

LEAST SQUARE TECHNIQUE TO FIND THE VALUES
OF k_1 AND k_2 FOR BEST DATA FITTED

$$\frac{1}{r''} = \frac{1}{k_2} \frac{1}{\{H_2O_2\}} + \frac{1}{k_1} \frac{1}{\{H^+\}} \quad A.2.1$$

which is of the form

$$y = a_1 x_1 + a_2 x_2 \quad A.2.2$$

If y_{mi} is the measured value of the dependent variable for a certain pair of values of the independent variables x_{1i} , x_{2i} , then the objective is to find values of a_1 and a_2 which minimize the sum of the squares of the deviation between the values of y as determined from equation A.2.2 and those measured thus:

$$\sum (y_i - y_{mi})^2 \text{ must be a minimum}$$

or

$$\sum \{(a_1 x_{1i} + a_2 x_{2i}) - y_{mi}\}^2 \text{ must be a minimum,}$$

This then requires that

$$a_1 \sum_{i=1}^N (x_{1i})^2 + a_2 \sum_{i=1}^N (x_{1i} x_{2i}) = \sum_{i=1}^N (y_{mi} x_{1i}) \quad A.2.3$$

and

$$a_1 \sum_{i=1}^N (x_{1i} x_{2i}) + a_2 \sum_{i=1}^N (x_{2i})^2 = \sum_{i=1}^N (y_{mi} x_{2i}) \quad \text{A.2.4}$$

These two equations have to be solved simultaneously for a_1 and a_2 . The limit N of the summation refers to the number of points to which the equation is to be fitted. In order to obtain a solution for a_1 and a_2 , N must be at least equal to 2.

```

5 REM PROGRAM TO CALCULATE THE BEST VALUES
6 REM OF K1 AND K2 TO FIT THE EXPERIMENTAL DATA
7 REM BY LEAST SQUARES TECHNIQUE
8 WRITE (8,*)"X(1)=(H2O2) MOL/LITER"
9 WRITE (8,*)"Z(1)=(H+) MOL/LITER"
10 WRITE (8,*)"Y(1)=MEASURED RATE MOL CU++·MIN-1·CM-2"
11 WRITE (8,*)"W= FITTED AND PREDICTED RATE,MOLCU++·MIN-1·CM-2"
12 WRITE (8,*)"P=% DEVIATION"
19 DIM X(20),Y(20),Z(20)
20 MAT C=ZER(2,2)
30 MAT E=ZER(2,2)
40 MAT A=ZER(2,1)
50 MAT D=ZER(2,1)
60 READ N,M
70 DATA 18,17
80 DATA 2.92,0.235,0.07,3.79,0.235,0.122,4.43,0.235,0.228
90 DATA 5.04,0.235,0.438,3.59,0.353,0.07,6.01,0.353,0.228
100 DATA 6.87,0.353,0.438,7.59,0.353,0.649,3.83,0.471,0.07
110 DATA 4.24,0.471,0.102,5.02,0.471,0.122,5.98,0.471,0.165
120 DATA 7.21,0.471,0.228,7.37,0.471,0.228,9.05,0.471,0.438
125 DATA 8.99,0.471,0.438,10.26,0.471,0.86,10.12,0.471,0.86
130 C1=C2=C3=S1=S2=0
140 FOR I=1 TO N
150 READ Y[I],X[I],Z[I]
160 Y1=1/Y[I]/1E-05
170 X1=1/X[I]
180 X2=1/Z[I]
190 C1=C1+Y1*X1
200 C2=C2+Y1*X2
210 C3=C3+X1*X2
220 S1=S1+X1^2
230 S2=S2+X2^2
240 NEXT I
250 C[1,1]=S1
260 C[1,2]=C3
270 C[2,1]=C3
280 C[2,2]=S2
290 D[1,1]=C1
300 D[2,1]=C2
310 MAT E=INV(C)
320 MAT A=E*D
330 A[1,1]=1/A[1,1]
340 A[2,1]=1/A[2,1]
350 WRITE (8,*)"K1=";A[2,1];"M·CU++·CM-2·MIN-1/(M·L-1 H+)"
360 WRITE (8,*)"K2=";A[1,1];"M·CU++·CM-2·MIN-1/(M·L-1 H2O2)"
370 WRITE (8,*)
380 WRITE (8,480)
390 WRITE (8,490)
400 FOR I=1 TO N
410 W=A[1,1]*A[2,1]*Z[I]*X[I]/(A[1,1]*X[I]+A[2,1]*Z[I])

```

```
420 Y1=Y[I]*1E-05
430 P=(Y1-W)/Y1*100
440 W=W*1E+05
450 WRITE (8,470)X[I],Z[I],Y[I],W,P
460 NEXT I
470 FORMAT F6.3,5X,F6.3,5X,F6.2,10X,F6.2,5X,F6.2
480 FORMAT 1X,"(H2O2)",6X,"(H+)",5X,"MEAS. RATE",6X,"FITTED RATE"
485 FORMAT 3X,"ERROR"
490 FORMAT 2X,"M./L",7X,"M./L",9X,"M. CU++. CM-2. MIN-1",10X,"Z"
500 WRITE (8,*)
510 WRITE (8,*)
515 WRITE (8,516)
516 FORMAT 39X,"PRED. RATE"
520 FOR I=1 TO M
530 READ Y[I],X[I],Z[I]
540 W=A[1,I]*A[2,I]*Z[I]*X[I]/(A[1,I]*X[I]+A[2,I]*Z[I])
550 Y1=Y[I]*1E-05
560 P=(Y1-W)/Y1*100
570 W=W*1E+05
580 WRITE (8,470)X[I],Z[I],Y[I],W,P
590 NEXT I
600 DATA 2.34,0.118,0.07,2.92,0.235,0.07,3.59,0.353,0.07
610 DATA 3.83,0.471,0.07,4.02,0.588,0.07,3.59,0.235,0.122
620 DATA 5.02,0.471,0.122,6.39,0.588,0.122,6.26,0.706,0.122
630 DATA 7.58,1.249,0.122,4.43,0.235,0.228,6.01,0.353,0.228
640 DATA 7.21,0.471,0.228,7.37,0.471,0.228,8.62,0.706,0.228
645 DATA 9.27,0.941,0.228,10.86,1.353,0.228
650 END
```

X(1)=(H2O2) MOL/LITER

Z(1)=(H+) MOL/LITER

Y(1)=MEASURED RATE MOL CU⁺⁺.MIN⁻¹.CM⁻²

W= FITTED AND PREDICTED RATE, MOL CU⁺⁺.MIN⁻¹.CM⁻²

P=% DEVIATION

K1= 7.90770E-04 M.CU⁺⁺.CM⁻².MIN⁻¹/(M.L-1 H⁺)

K2= 2.53171E-04 M.CU⁺⁺.CM⁻².MIN⁻¹/(M.L-1 H2O2)

(H2O2) M./L	(H+) M./L	MEAS.RATE M.CU ⁺⁺ .CM ⁻² .MIN ⁻¹	FITTED RATE	ERROR %
0.235	0.070	2.92	2.87	1.80
0.235	0.122	3.79	3.68	2.90
0.235	0.228	4.43	4.47	-0.98
0.235	0.438	5.04	5.08	-0.74
0.353	0.070	3.59	3.42	4.79
0.353	0.228	6.01	5.98	0.58
0.353	0.438	6.87	7.10	-3.41
0.353	0.649	7.59	7.61	-0.28
0.471	0.070	3.83	3.78	1.29
0.471	0.102	4.24	4.81	-13.48
0.471	0.122	5.02	5.33	-6.23
0.471	0.165	5.98	6.23	-4.19
0.471	0.228	7.21	7.18	0.45
0.471	0.228	7.37	7.18	2.61
0.471	0.438	9.05	8.87	1.98
0.471	0.438	8.99	8.87	1.33
0.471	0.860	10.26	10.15	1.12
0.471	0.860	10.12	10.15	-0.25

			PRED. RATE	
0.118	0.070	2.34	1.94	17.08
0.235	0.070	2.92	2.87	1.80
0.353	0.070	3.59	3.42	4.79
0.471	0.070	3.83	3.78	1.29
0.588	0.070	4.02	4.04	-0.37
0.235	0.122	3.59	3.68	-2.51
0.471	0.122	5.02	5.33	-6.23
0.588	0.122	6.39	5.85	8.39
0.706	0.122	6.26	6.27	-0.09
1.249	0.122	7.58	7.39	2.48
0.235	0.228	4.43	4.47	-0.98
0.353	0.228	6.01	5.98	0.58
0.471	0.228	7.21	7.18	0.45
0.471	0.228	7.37	7.18	2.61
0.706	0.228	8.62	8.98	-4.13
0.941	0.228	9.27	10.26	-10.71
1.353	0.228	10.86	11.81	-8.77

REFERENCES

1. Riddiford, A.C., and Bircumshaw, M.A., Transport control in heterogeneous reactions: Quarterly Reviews, no. 6, p. 157 (1952)
2. Burkin, A.R., The chemistry of hydrometallurgical processes: Princeton, New Jersey, D. van Nostrand, Inc., (1965).
3. Habashi, F., Extractive metallurgy: v. 1, Gordon and Breach Science Publishers (1969)
4. Gatos, H.C., and Lavine, M.C., Progress in semiconductors: London, Heywood (1965).
5. Bockris, J. O'M., Leddy, A.K., Modern electrochemistry: v. 2, New York, Plenum/Rosetta (1973).
6. Gregory, D.P., Riddiford, A.C., Transport to the surface of a rotating disk: Jour. Chem. Soc., p. 3756-64 (1956).
7. Gregory, D.P., Riddiford, A.C., Dissolution of copper in sulfuric acid solutions: Jour. Electrochem. Soc., p. 950-56 (1960).
8. Zembura, Z., Fulinski, A., Rotating disk investigations of kinetics of metal dissolution: case of two independent dissolution reactions.: Electrochem. Acta, p. 859-65 (1965)
9. Zembura, Z., Ziolkowska, W., The kinetics of reduction of oxygen at the surface of iron corroding in acidic Na_2SO_4 solutions: Roczniki Chemii, p. 1054-62 (1966).
10. Zembura, Z., Glodzinska, W., Kinetics of copper dissolution. I. Reaction regions in oxygen-saturated solutions of Na_2SO_4 at various pH: Roczniki Chemii, p. 911-17 (1966)⁴
11. Zembura, Z., Glodzinska, W., Part II. Reaction regimes in 0.1M solution of H_2SO_4 at temperatures 5-75°C: Roczniki Chemii, p.1525-15 (1968).

12. Perez, V., Thermodynamic and kinetic considerations in the hydrogen reduction of nickel from ammonical solutions: Golden, Colo., Colo. School of Mines, MSc Thesis (1973).
13. Levich, V., Physicochemical hydrodynamics: New Jersey, Prentice Hall, Inc. (1962).
14. Habashi, F., Kinetics of corrosion of metals: Jour. of Chem. Educ., p. 319-22 (1965).
15. Wadsworth, M., Reduction of metals in solution: Trans. Metallur. Soc. AIME, p. 1381-93 (1969).
16. Labergere, J., Pickling of copper and brass: Wire Jour., p. 190-200 (1967).
17. Wilmotte, R., and Benezech, J., Le Decapage: Galvano, p. 335-42 (1973).
18. Winkley, D.C., Grand, A.F., Hydrogen peroxide pickling of copper rod: Wire Journal, p. 64-49 (Aug. 1973).
19. Wadsworth, M., Principles of hydrometallurgy, short course by TSM, (1973).
20. Gatos, H.C., The surface chemistry of metals and semi-conductors: New York, John Wiley & Sons (1959).
21. Peters, E., Theory of leaching: lecture notes on hydrometallurgy: theory and practice (1972)
22. King, C.V., Abramson, M., The rate of dissolution of iron in acids: Jour. A. Chem. Soc., p. 2290-95 (1937).
23. Balberyszski, T., Effect of pressure on the kinetics of dissolution of metals in aqueous iodine solutions: Golden, Colo., Colo. School of Mines, Ph.D. Thesis (1972).
24. Krebs, R., Dissolution kinetics of copper in hydrochloric acid: Golden, Colo., Colo School of Mines, M.Sc. Thesis (1972).
25. Pourbaix, M., Atlas of electrochemical equilibria in aqueous solutions: Pergamon Press, (1966).
27. Joksimovic-Tjapkin, S., and Delic, D., Kinetics of concentrated hydrogen peroxide decomposition on a rotating silver disk: Industrial Eng. Chem. Fundam., v. 12, p. 33-39 (1973).

28. Baxendale, J.H., Decomposition of hydrogen peroxide by catalysts in homogeneous aqueous solutions: *Advances in Catalysis*, V. 4, New York, Academic Press Inc., (1952).
29. Barb, W.G., Baxendale, J.H., George, P., and Hargrave, K.R., Reactions of ferric ions with H_2O_2 : *Trans. Faraday Society*, p. 591-616 (1951)
30. Lewis, T.J., Behavior of stannic acid sols. in concentrated H_2O_2 : *J. Appl. Chem.*, p. 396-407 (1960).
31. Young, T.F. and Blatz, L.A., The variation of the properties of electrolytic solutions with degrees of dissociation: *Chemical Review*, V. 44, p. 102 (1949)
32. Hauffe, von K. and Reinhold, Über die auflösung von kupfer (I)-oxid - einkristallen in verdünnter schwefelsäure: *Berichte Der Bunsen- Gesellschaft*, p. 616-621 (1972).
33. Colcleugh, D.W., and Grayson, W.F., Hydrogen peroxide oxidation of cuprous ion: *Canadian Jour. of Chem.*, p. 1497 (1962).
34. Wadsworth, M., and Wadia, D., Reaction rate study of the dissolution of cuprite in sulphuric acid: *Trans. AIME*, p. 755-759 (1955).
35. Shumb and Hoja, G., *Hydrogen Peroxide*: New York, Reinhold Publishing Corporation (1955)
36. Leidheiser, H., *The corrosion of copper, tin, and their alloys*: John Wiley and Sons, Inc. (1971)